




## Dark-time decay of the retrieval efficiency of light stored as a Rydberg excitation in a noninteracting ultracold gas

Steffen Schmidt-Eberle , Thomas Stolz, Gerhard Rempe, and Stephan Dürr   
*Max-Planck-Institut für Quantenoptik, Hans-Kopfermann-Strasse 1, 85748 Garching, Germany*

 (Received 2 September 2019; revised manuscript received 4 December 2019; published 14 January 2020)

We study the dark-time decay of the retrieval efficiency for light stored in a Rydberg state in an ultracold gas of  $^{87}\text{Rb}$  atoms based on electromagnetically induced transparency (EIT). Using low atomic density to avoid dephasing caused by atom-atom interactions, we measure a  $1/e$  time of  $30\ \mu\text{s}$  for the  $80S$  state in free expansion. One of the dominant limitations is the combination of photon recoil and thermal atomic motion at  $0.2\ \mu\text{K}$ . If the  $1064\text{-nm}$  dipole trap is left on, then the  $1/e$  time is reduced to  $13\ \mu\text{s}$ , in agreement with a model taking differential light shifts and gravitational sag into account. To characterize how coherent the retrieved light is, we overlap it with reference light and measure the visibility  $V$  of the resulting interference pattern, obtaining  $V > 90\%$  for short dark time. Our experimental work is accompanied by a detailed model for the dark-time decay of the retrieval efficiency of light stored in atomic ensembles. The model is generally applicable for photon storage in Dicke states, such as in EIT with  $\Lambda$ -type or ladder-type level schemes and in Duan-Lukin-Cirac-Zoller single-photon sources. The model includes a treatment of the dephasing caused by thermal atomic motion combined with net photon recoil, as well as the influence of trapping potentials. It takes into account that the signal light field is typically not a plane wave. The model maps the retrieval efficiency to single-atom properties and shows that the retrieval efficiency is related to the decay of fringe visibility in Ramsey spectroscopy and to the spatial first-order coherence function of the gas.

DOI: [10.1103/PhysRevA.101.013421](https://doi.org/10.1103/PhysRevA.101.013421)

### I. INTRODUCTION

Decay of coherence is a major performance-limiting factor in photonic quantum memories [1]. Among the various schemes for such memories, the focus of the present work is on storage and retrieval of light [2–5] in an ultracold atomic ensemble based on electromagnetically induced transparency (EIT) [6]. The storage produces a spin wave in the atomic ensemble. Various physical effects cause the coherence of the spin wave to decay as a function of the dark time between storage and retrieval. As a result, the efficiency of the retrieval decays. Over the years, various techniques have been used to extend the decay time. For ground-state EIT in ultracold atomic gases, a  $1/e$  time of  $16\ \text{s}$  was reached a few years ago [7].

Aiming at the creation of strong interactions between photons, EIT has been combined with Rydberg states [8–10]. Coherence in Rydberg EIT suffers from the fact that the sensitivity of a Rydberg atom to interactions with surrounding ground-state atoms increases with atomic density and with increasing principal quantum number [11–14]. In addition, when the atoms are held in a red-detuned optical dipole trap, the differential light shifts between the ground and Rydberg state are large. To avoid light shifts, many experiments are carried out in free expansion. In recent experiments on Rydberg EIT, the  $1/e$  decay time has been pushed to  $12\ \mu\text{s}$  for the  $45S$  state in free expansion [14] and to approximately  $20\ \mu\text{s}$  for the  $65S$  state in a magic-wavelength optical lattice specifically designed to fight decoherence [15].

We recently demonstrated a photon-photon quantum gate based on Rydberg interactions [16]. The gate required a fairly

high atomic density of  $2 \times 10^{12}\ \text{cm}^{-3}$  because light had to accumulate a  $\pi$  phase shift in a single pass through the blockade volume. Correspondingly, atom-atom interactions caused a decay of coherence on a timescale of a few microseconds, which was the key limiting factor for the overall performance of the gate. Much better performance of a photon-photon gate should be achievable using Rydberg blockade in an atomic ensemble inside an optical resonator of moderate finesse (Rydberg cavity gate) [17–19] because, among other things, light passing many times through a blockade volume can accumulate a large effect even at low atomic density, where decoherence should be much slower.

Here, we present an experiment in which we extend the  $1/e$  decay time of Rydberg EIT retrieval from the  $80S$  state in  $^{87}\text{Rb}$  to  $30\ \mu\text{s}$  in free expansion. This is achieved by operating at a low peak atomic density of  $5 \times 10^{10}\ \text{cm}^{-3}$  to make atom-atom interactions negligible and at a low temperature of  $0.2\ \mu\text{K}$  to reduce the effect of net photon recoil. We combine this with an experimental study of the dependence of the decay time on temperature. In addition, we overlap the retrieved light with a local oscillator and measure a visibility above  $90\%$ . This is a considerable improvement over the  $66\%$  visibility that we previously measured at a peak density of  $2 \times 10^{12}\ \text{cm}^{-3}$  [16]. If the dipole trap with a wavelength of  $1064\ \text{nm}$  is left on during the experiment, the  $1/e$  decay time is reduced to  $13\ \mu\text{s}$ .

Our experimental work is accompanied by a theoretical analysis of the decay of the EIT retrieval efficiency for light stored in a gas of noninteracting atoms. The model is applicable to EIT-based storage in  $\Lambda$ -type or ladder-type level schemes. The retrieval efficiency can be calculated from

single-particle properties. We show that the resulting expressions are analogous to expressions for the decay of the fringe visibility in Ramsey spectroscopy as a function of dark time. We also note that the EIT retrieval decay is equivalent to the decay of the read efficiency in single-photon sources based on the inherently probabilistic Duan-Lukin-Cirac-Zoller (DLCZ) protocol [20]. In addition, we show that when applying the model to photon recoil during storage combined with thermal atomic motion, the decay of retrieval efficiency can be regarded as a direct experimental probe of the spatial first-order coherence function of the gas.

We apply this model to study several scenarios: (i) photon recoil during storage combined with thermal atomic motion [13,21–23], (ii) a harmonic differential light-shift potential [15,23–26], and (iii) release from a harmonic trap [23]. According to the model, photon recoil combined with thermal motion is one of the dominant limitations for the observed  $1/e$  time of  $30 \mu\text{s}$ . This model also agrees well with the temperature dependence of the decay time measured here. The observed reduction of the  $1/e$  time to  $13 \mu\text{s}$  in the dipole trap is explained by the model when taking into account the differential light shift and the gravitational sag of the atomic cloud in the trapping potential. The model predicts that producing the same harmonic trapping potential with 532-nm light should make the light-shift contribution to the decay irrelevant compared to the presently observed  $30 \mu\text{s}$ .

This paper is organized as follows. In Sec. II we present experimental results and compare with results from a model. This model is introduced in Sec. III and applied to several experimentally relevant situations in Sec. IV.

## II. EXPERIMENT

This section presents experimental results of the decay of the retrieval efficiency during the dark time. It begins with a description of the experimental setup and procedure in Sec. II A, which is followed by Sec. II B presenting an experimental study of the decay of the retrieval efficiency in free expansion. The results agree largely with results from a model taking into account photon recoil combined with thermal atomic motion. In Sec. II C we observe that the decay becomes faster if the optical dipole trap is left on during the dark time. In Sec. II D we investigate to which degree the retrieved light is coherent.

### A. Experimental procedure

Our experiment is based on a double magneto-optical trap (MOT) system.  $^{87}\text{Rb}$  atoms are collected in a first MOT from a background vapor and then transferred to a second MOT at much lower background pressure. After polarization-gradient cooling and optical pumping, the atoms are transferred into a Ioffe-Pritchard magnetic trap. Radiofrequency (rf) induced evaporative cooling in the magnetic trap allows it to reach sub-microkelvin temperatures. The atoms are finally transferred into an optical dipole trap. In the past, we produced BECs in this apparatus [27]. In recent years, however, we have used the apparatus to study Rydberg EIT, for which the high atomic density in a BEC of typically  $10^{14} \text{ cm}^{-3}$  is disadvantageous because atom-atom interactions would produce fast

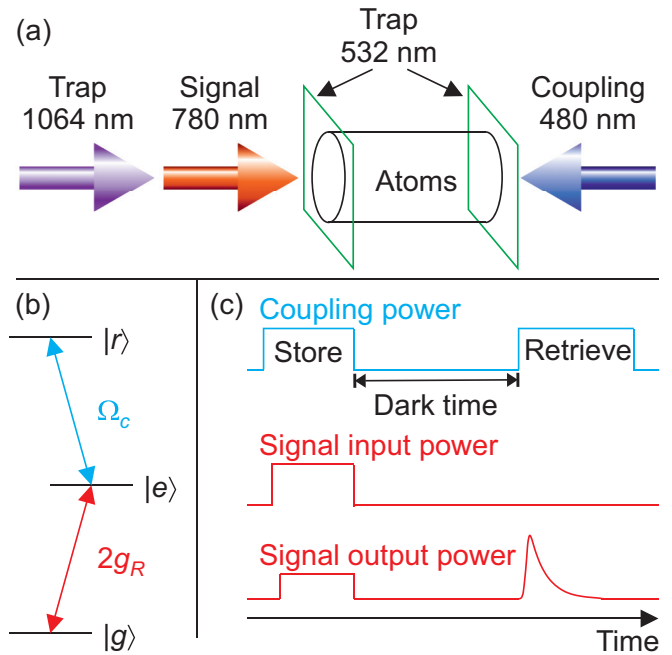


FIG. 1. (a) Scheme of the beam geometry. Trapping light at 1064 nm creates a radially confining optical dipole trap for the atomic ensemble. 532 nm light sheets provide a boxlike longitudinal optical dipole potential. 780 nm signal light copropagates with the 1064 nm trapping light. 480 nm EIT coupling light counterpropagates the signal light to minimize the net photon recoil in the two-photon transition  $|g\rangle \leftrightarrow |r\rangle$ . (b) Scheme of the atomic levels and transitions. A weak signal light field with vacuum Rabi frequency  $2g_R$  drives the transition  $|g\rangle \leftrightarrow |e\rangle$ . Strong EIT coupling light with Rabi frequency  $\Omega_c$  drives the transition  $|e\rangle \leftrightarrow |r\rangle$ . (c) Scheme of the timing sequence. The storage pulse consists of incoming signal and coupling light. Storage of the signal light is achieved by switching off the coupling light. Because of imperfections, some signal light leaks through the atomic ensemble, thus appearing at the output with some group delay. The storage is followed by a dark time, after which the coupling light is switched back on. This causes the stored signal light to be retrieved.

dephasing; see, e.g., Ref. [12]. To avoid this, we operate at much lower atomic densities. Technically, we achieve this by deliberately loading much fewer atoms than possible. As a result, the typical temperatures of a few hundred nanokelvin are far above quantum degeneracy.

The dipole trap is made of a horizontally propagating light beam with a wavelength of 1064 nm and a beam waist ( $1/e^2$  radius of intensity) of  $140 \mu\text{m}$ ; see Fig. 1(a). At a power of 3.7 W, the trap depth is estimated to be  $k_B \times 18 \mu\text{K}$ , where we used the dynamical polarizability of the ground state at 1064 nm of 687.3 a.u. [28]. Here,  $k_B$  is the Boltzmann constant, and one atomic unit is  $1.649 \times 10^{-41} \text{ J}/(\text{V}/\text{m})^2$ . This beam provides a radial confinement with a harmonic trapping frequency of  $\omega/2\pi = 96 \text{ Hz}$  estimated from the beam waist and power. This agrees fairly well with the measured value of 87(8) Hz. The axial confinement resulting from the divergence of the 1064 nm beam is estimated to be below 0.1 Hz, which is negligible. The gravitational acceleration of  $g = 9.8 \text{ m}/\text{s}^2$  causes a gravitational sag of  $x_{g,s} = g/\omega^2 = 27 \mu\text{m}$ . In the

radial direction, the one-dimensional (1D) root-mean-square (rms) radius is  $\sigma_x = \sqrt{k_B T / m \omega^2}$ , where  $m$  is the atomic mass, yielding, e.g.,  $\sigma_x = 7 \mu\text{m}$  for  $T = 0.2 \mu\text{K}$ .

In the axial direction, a boxlike potential is produced using two light sheets at a wavelength of 532 nm with beam waists of  $55 \mu\text{m}$  along gravity and  $14 \mu\text{m}$  orthogonal thereto, similar to Ref. [16]. Adjusting the power of the 532 nm light sheets allows for evaporative cooling in the dipole trap without changing the radial confinement provided by the 1064 nm light. The resulting temperature depends on the power of the light sheets. The separation of the centers of the light sheets is typically 0.43 mm. Combining this number with the temperature and with the dynamical polarizability of  $-250$  a.u. [29] for the ground state at 532 nm, we can estimate the length of the medium  $L$  (full width at half-maximum).

For example, for  $T = 0.2 \mu\text{K}$  and a typical power of 25 mW for each light sheet we estimate  $L = 0.40$  mm. Combining this with an atom number of, e.g.,  $N = 1 \times 10^4$  yields a peak atomic density of  $\rho_0 = 8 \times 10^{10} \text{ cm}^{-3}$  and a peak phase space density of  $\rho_0 \lambda_{\text{dB}}^3 = 6 \times 10^{-3}$ , where  $\lambda_{\text{dB}} = \hbar \sqrt{2\pi / mk_B T}$  is the thermal de Broglie wavelength. As  $\rho_0 \lambda_{\text{dB}}^3 \ll 1$ , the temperature is far above quantum degeneracy.

The atomic sample is prepared in the stretched spin state  $|g\rangle = |5S_{1/2}, F = m_F = 2\rangle$  of the atomic ground state, where  $F, m_F$  are the hyperfine quantum numbers. The quantization axis is chosen along the wave vector of the 1064-nm light beam. A magnetic field of  $24 \mu\text{T}$  applied along the quantization axis preserves the spin preparation of the sample.

The sample can be illuminated with an EIT signal-light beam with a beam waist of  $w = 8 \mu\text{m}$  and a wavelength of  $\lambda_{\text{eg}} = 780.24$  nm, resonantly driving the  $|g\rangle \leftrightarrow |e\rangle$  transition, where  $|e\rangle = |5P_{3/2}, F = m_F = 3\rangle$ . A scheme of the atomic levels and transitions is shown Fig. 1(b). The EIT signal-light beam copropagates with the 1064 nm dipole trapping beam. In addition, the sample can be illuminated with an EIT coupling-light beam with a beam waist of  $29 \mu\text{m}$  and a wavelength of  $\lambda_{\text{re}} = 480$  nm, resonantly driving the  $|e\rangle \leftrightarrow |r\rangle$  transition, where  $|r\rangle = |nS_{1/2}, F = m_F = 2\rangle$  is a Rydberg state with principal quantum number  $n$ . The EIT coupling-light beam counterpropagates the EIT signal-light beam to minimize the net photon recoil of the two-photon transition from  $|g\rangle$  to  $|r\rangle$ . Note that the states  $|g\rangle$  and  $|r\rangle$  experience, to a good approximation, the same linear Zeeman effect.

We use the following timing sequence, schematically shown in Fig. 1(c), to achieve EIT-based storage and retrieval of the signal light. First, the EIT coupling light is turned on. Next, a pulse of EIT signal light is sent onto the sample. The incoming EIT signal pulse has a rectangular temporal shape. Unless otherwise noted, its duration is  $0.5 \mu\text{s}$ . Because of EIT, the signal light becomes a Rydberg polariton when inside the sample. The pulse experiences a much-reduced group velocity, which causes a drastic spatial compression of the pulse in the longitudinal direction upon entering the sample [6]. When the signal pulse is inside the medium, the coupling light is switched off. Hence, the signal light is converted into a stationary Rydberg excitation [2,3]. After a variable dark time  $t$ , the coupling light is switched back on. This couples the population in state  $|r\rangle$  to the state  $|e\rangle$  from where spontaneous emission into state  $|g\rangle$  can occur. There is interference between the light emitted from the large number

of atoms in the ensemble. Ideally, the interference is such that the signal light pulse resumes propagation with an unchanged form of the longitudinal and transverse wave packet. This retrieval can, to a good approximation, be regarded as the time-reversed process of the storage.

In practice, various physical effects can cause deviations from this ideal retrieval scenario. While a possible change in the longitudinal wave packet could, in principle, be compensated by shaping the temporal profile of the coupling light pulse during retrieval, a change in the transverse profile is typically hard to compensate. Hence, the fraction  $\eta$  of the incoming light which is emitted into the original transverse mode is an important figure of merit.  $\eta$  is the combined efficiency of the storage-and-retrieval process. For brevity, we refer to  $\eta$  as the retrieval efficiency throughout this work. To measure  $\eta$ , we focus the light emitted from the atomic sample into a single-mode optical fiber and measure the light intensity behind the fiber. In the absence of the atomic ensemble, we achieve a fiber-coupling efficiency of 45% for coupling the signal light, impinging at the position where the atoms would usually be, into the optical fiber. In our present work, we are not interested in the retrieval efficiency  $\eta$  at short dark time. Instead, we focus on the decay of the retrieval efficiency  $\eta$  as a function of the dark time  $t$  between storage and retrieval.

The incoming EIT signal pulse is derived from a continuous-wave laser using an acousto-optical modulator for pulse shaping. To a good approximation, it can be modeled as a coherent state with a Poissonian photon number distribution. The average number of photons is approximately one. Hence, the probability of having more than one incoming photon is not negligible. Nonetheless, the probability that two stored Rydberg excitations interact with each other during the dark time is negligible. This is partly because the storage efficiency is fairly low, typically between 10% and 20%, and partly because the spatial compression of the EIT signal pulse inside the medium is moderate, giving it a length of several hundreds of micrometers, which is large compared to the radius over which the van der Waals interaction between two stationary Rydberg excitations is noticeable.

To avoid decay of  $\eta$  resulting from the differential light shifts created by the dipole trapping potential, we switch the dipole trap off before sending the EIT signal light pulse into the sample. Hence, each storage-and-retrieval experiment takes place during free expansion. As the preparation of the atomic sample is time-consuming, we perform many repetitions of the experiment on the same atomic sample. To do so, we recapture the atomic ensemble by switching the dipole trap back on  $35 \mu\text{s}$  after switching it off. This is well after the retrieval is over.

The number of repetitions that we can perform on one sample is limited by heating caused, first, by spontaneous emission of 780 nm photons that were absorbed because of imperfect EIT, and secondly, and most importantly, by periodically switching the dipole trapping light on and off. We choose to perform 1000 repetitions of the experiment for each atomic sample. During the course of these 1000 repetitions for one atomic sample, we typically observe a 20% increase in temperature. Because of spontaneous evaporation over the 532-nm light sheet barriers, this is accompanied by a 20% decrease in atom number. We separate these repetitions by

1 ms from one another. On the one hand, this gives possibly left-behind Rydberg excitations time to decay spontaneously to the ground state. On the other hand, this means that the 35  $\mu\text{s}$  during which the trap is off has a negligible time-averaged effect. So, the 1000 repetitions take a total time of 1 s, after which we prepare a new atomic sample, which takes between 13 and 19 s depending on the choice of the final temperature. Clearly, it would be desirable to avoid the periodic release and recapture because without it, the heating would be much reduced, allowing it to perform typically ten times as many repetitions of the experiment before needing to prepare a new atomic sample. This would increase the time-averaged data acquisition rate by an order of magnitude when choosing the separation between repetitions to 100  $\mu\text{s}$  as in Ref. [16].

Compared to our previous experiments [16], we operate at lower atomic density, which increases the group velocity for the EIT signal light pulse. Hence, a lower EIT coupling Rabi frequency would be needed to achieve a similar group velocity. This is partly compensated by the longer medium for which a somewhat higher group velocity is needed for optimal storage efficiency. We choose the power of the EIT coupling beam to be between 5 and 25 mW depending on atomic density and principal quantum number. The EIT coupling Rabi frequency ranges between 3 and 12 MHz. The repulsive potential that the 480 nm EIT coupling light causes for the ground-state atoms has a negligible effect because it is typically on only 0.3% of the time, similar to Refs. [12,16].

### B. Decay caused by photon recoil combined with thermal motion

An important mechanism that causes decay of the retrieval efficiency is thermal atomic motion combined with the net photon recoil  $\hbar k_R$  transferred during storage on the two-photon transition from  $|g\rangle$  to  $|r\rangle$ . According to Eq. (51), this mechanism is expected to cause a decay of the retrieval efficiency governed by

$$\frac{\eta(t)}{\eta(0)} = e^{-t^2/\tau_R^2}, \quad \tau_R = \frac{1}{k_R} \sqrt{\frac{m}{k_B T}}. \quad (1)$$

Hence,  $\eta(t)$  is expected to exhibit a Gaussian decay as a function of dark time  $t$  with  $1/e$  time  $\tau_R$ .

To test the prediction of a Gaussian decay, we consider the measurement of  $\eta$  as a function of  $t$  displayed in Fig. 2. The data span from  $t = 0.7$  to 31.5  $\mu\text{s}$ . The line is a fit of the Gaussian decay from Eq. (1) to the data. The vertical axis in the figure is logarithmic and the horizontal axis shows  $t^2$ . With these axes, the Gaussian decay becomes a straight line. The fit agrees well with the data. To analyze the data in Fig. 2 from a different perspective, we fit  $\eta(t) = \eta(0) \exp[-(t/\tau)^p]$  with free fit parameters  $p$ ,  $\tau$ , and  $\eta(0)$  to these data, obtaining the best-fit value  $p = 2.0(1)$ . Again, this shows that a Gaussian models the situation well.

For comparison, Ref. [21] observed an exponential decay of the retrieval efficiency for ground-state EIT in an uncondensed cloud of sodium atoms with a  $1/e$  time that is a factor of 0.7 shorter than the expectation from Eq. (1). It is difficult to explain this in hindsight without performing additional experimental tests on that setup.

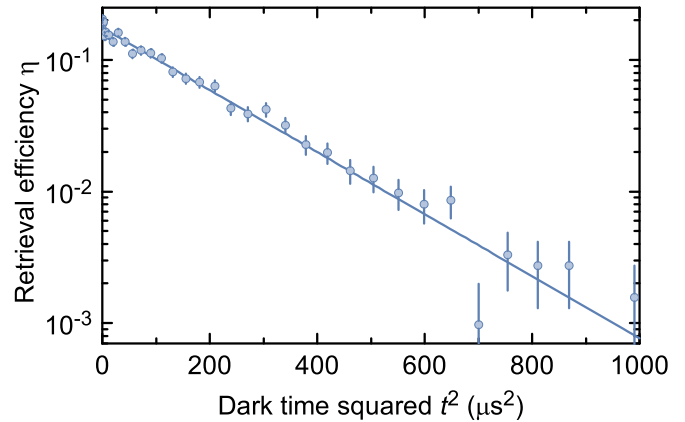


FIG. 2. Retrieval efficiency  $\eta$  as a function of the square of the dark time  $t$  for the 70S state at  $T = 2.0 \mu\text{K}$  in free expansion. The data cover two orders of magnitude in  $\eta$ . The line is a fit of a Gaussian decay according to Eq. (1), which agrees well with the experimental data. With a logarithmic vertical axis and  $t^2$  on the horizontal axis, the fit curve is a straight line.

To study how the  $1/e$  time  $\tau$  extracted from the fit depends on temperature  $T$ , we record a series of data sets similar to the one shown in Fig. 2 and extract  $\tau$  by fitting the Gaussian of Eq. (1) to each data set. The resulting values of  $\tau$  are shown in Fig. 3. The data cover an order of magnitude in  $T$ . Different symbols represent different principal quantum numbers. The rightmost data point for the 70S state represents the data set from Fig. 2.

To change the temperature, we varied the power of each light sheet between 25 and 320 mW. We estimate  $L$

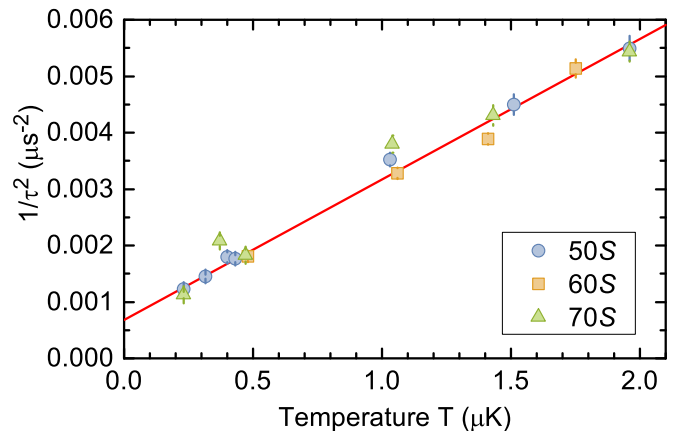


FIG. 3. Inverse decay time squared  $1/\tau^2$  of the retrieval efficiency in free expansion as a function of temperature  $T$ . Data points with different symbols correspond to different principal quantum numbers  $n$ . There is no discernible dependence on  $n$  in the parameter range studied here. According to Eq. (1), all data in this figure are expected to fall onto a straight line through the origin. A straight-line fit to all data yields a slope that agrees well with the expectation from Eq. (1). For small  $T$ , the fit reveals an additional decay mechanism of presently unclear origin. Extrapolating the straight line to  $T = 0$  yields  $\tau = 38(2) \mu\text{s}$ . The in-trap peak atomic density is  $\rho_0 \leq 1.7 \times 10^{11} \text{ cm}^{-3}$  for all these data so that atom-atom collisions are negligible.

between 0.39 and 0.40 mm and  $\varrho_0$  between  $5 \times 10^{10}$  and  $1.7 \times 10^{11} \text{ cm}^{-3}$  for all data in Figs. 2 and 3. By varying the atomic density in additional measurements not shown here, we experimentally verified that for these principal quantum numbers, a density dependence of  $\tau$  appears only for noticeably higher density, which means that atom-atom interactions have a negligible effect in Figs. 2 and 3.

As Fig. 3 shows  $1/\tau^2$  versus  $T$ , Eq. (1) predicts that all data should fall onto a straight line through the origin. The line in Fig. 3 is a straight-line fit to the data. The fit agrees well with the data. The slope can be expressed in terms of a best-fit value for the wavelength of the spin wave  $\lambda_R = 2\pi/k_R = 1.23(3) \mu\text{m}$ . This agrees well with the  $\lambda_R = (\lambda_{re}^{-1} - \lambda_{eg}^{-1})^{-1} = 1.25 \mu\text{m}$  expected in the counterpropagating geometry of our experiment. Hence, for large enough  $T$  the temperature dependence of  $\tau$  agrees well with the prediction from Eq. (1).

In the limit  $T \rightarrow 0$ , however, the fit extrapolates to  $\tau = 38(2) \mu\text{s}$  instead of  $\tau \rightarrow \infty$  expected from Eq. (1). This indicates that there is an additional decay mechanism becoming relevant at low temperature. The physical origin thereof is presently unclear [30].

### C. Decay caused by dipole-trapping light

Another important mechanism that causes decay of the retrieval efficiency is a spatially inhomogeneous difference of the potentials experienced by states  $|g\rangle$  and  $|r\rangle$ . The 1064 nm dipole trapping light creates an attractive potential for the ground state with dynamical polarizability  $\alpha_g = 687.3 \text{ a.u.}$ ; see above. For the Rydberg state, the dynamical polarizability is well approximated by that of a free electron (see, e.g., Ref. [29]), yielding  $\alpha_r = -550 \text{ a.u.}$  at 1064 nm. If this light is left on during the experiment, this will cause a dark-time decay of  $\eta$  because the differential light shift depends on the atomic position.

To study the size of this effect, we recorded the experimental data shown in Fig. 4. While the blue circles represent data taken in free expansion after switching the trap off, the orange squares represent data taken in the dipole trap. A Gaussian fit according to Eq. (1) yields a  $1/e$  decay time of  $\tau = 30(1) \mu\text{s}$  for the free-expansion data. Clearly, the in-trap data decay much faster.

To model the in-trap decay time, we approximate the radial confinement produced by the 1064-nm light as harmonic, we assume that the sample is axially homogeneous, and we neglect the presence of the 532-nm light sheets. According to Eqs. (66) and (69), this yields an algebraic decay

$$\frac{\eta(t)}{\eta(0)} = \frac{1}{1 + t^2/\tau_\kappa^2}, \quad \tau_\kappa = \frac{4\hbar}{w_r^2|\kappa_g - \kappa_r|}, \quad (2)$$

where  $\kappa_g$  and  $\kappa_r$  are the spring constants of the harmonic potentials  $V_g(\mathbf{x}) = \frac{1}{2}\kappa_g(x^2 + y^2)$  and  $V_r(\mathbf{x}) = \frac{1}{2}\kappa_r(x^2 + y^2)$  experienced by atoms in states  $|g\rangle$  and  $|r\rangle$ , respectively, and the radial sizes are  $w = 8 \mu\text{m}$  for the signal beam waist,  $2\sigma_x = \sqrt{4k_B T/m\omega^2} = 14 \mu\text{m}$  for the ground-state atom cloud, and, according to Eq. (65),

$$w_r = \left( \frac{1}{4\sigma_x^2} + \frac{1}{w^2} \right)^{-1/2} \quad (3)$$

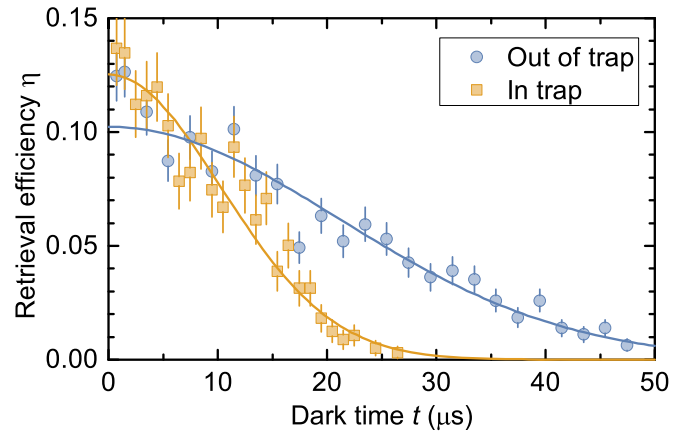


FIG. 4. Retrieval efficiency as a function of the dark time for the 80S state. Blue circles represent data taken after release from the trap. Orange squares represent data taken in the 1064-nm dipole trap. According to Eqs. (1) and (4), we expect a Gaussian decay in either case. Gaussian fits (lines) yield  $1/e$  times of  $\tau = 30(1)$  and  $12.5(6) \mu\text{s}$  with the trap off and on, respectively. Data were taken at a low temperature of  $0.2 \mu\text{K}$  to keep the dephasing rate caused by photon recoil combined with thermal motion small and at a low in-trap peak atomic density of  $5 \times 10^{10} \text{ cm}^{-3}$  to avoid dephasing caused by atom-atom interactions.

for that part of the atom cloud that was transferred into state  $|r\rangle$  during storage. Experiments on EIT-based storage and retrieval are typically operated in the regime  $w \ll 2\sigma_x$  because otherwise some part of the light would transversely miss the atomic ensemble, resulting in low storage efficiency. Hence, typically  $w_r \approx w$ .

As the differential potential  $V_r - V_g$  depends quadratically on the radial position in this model, it imprints a phase onto the retrieved light, which depends quadratically on the radial position. This is equivalent to inserting a lens. Hence, the dark-time decay of the amount of light coupled into the single-mode fiber is not caused by dephasing in the sense that the phase evolution of different atoms would fluctuate as a result of a fluctuating external parameter. Instead, this dark-time decay is caused by changing the focusing of the retrieved light. For fixed dark time, one could compensate this, in principle, by changing the alignment of the single-mode fiber.

For the parameters of Fig. 4, this model predicts a  $1/e$  time of  $\tau_\kappa \sqrt{e-1} = 120 \mu\text{s}$ . This would suggest that this additional mechanism for trap-induced decay should be negligible compared to the  $30 \mu\text{s}$  decay time from the free-expansion data. However, the experimental in-trap data clearly decay much faster.

This discrepancy is resolved when taking into account gravitational sag, i.e., the fact that gravity shifts the equilibrium position of the atomic cloud away from the center of the dipole trapping beam. As a result, the differential potential  $V_r - V_g$  between states  $|r\rangle$  and  $|g\rangle$  varies linearly in position when moving away from the cloud center, whereas in the absence of gravitational sag, it would vary quadratically. Hence, gravitational sag causes the finite-size atomic cloud to sample larger values of the differential potential.

In our experiment, the radius of the atomic cloud  $\sigma_x = 7 \mu\text{m}$  at  $T = 0.2 \mu\text{m}$  is much smaller than the gravitational

sag  $x_{g,s} = 27 \mu\text{m}$ . Hence, the curvature of the potential becomes negligible, and according to Eqs. (65) and (71) we expect  $\eta$  to decay as

$$\frac{\eta(t)}{\eta(0)} = \exp\left(-\frac{t^2}{\tau_F^2}\right), \quad \tau_F = \frac{2\hbar}{w_r|F|}, \quad (4)$$

where  $F = -\nabla(V_r - V_g)$  is the differential force, to be taken at the cloud center. Note that taking into account the finite size  $w_r$  of the atomic cloud transferred to state  $|r\rangle$  is crucial here, because in the limit  $w_r \rightarrow \infty$ , Eq. (4) yields  $\tau_F \rightarrow 0$ . The plausibility of this is discussed in Sec. IV D.

As the differential potential depends linearly on the position along gravity in this model, it imprints a phase onto the retrieved light that depends linearly on the position along gravity. This is equivalent to inserting a prism. Hence, the dark-time decay of the amount of light coupled into the single-mode fiber is not caused by dephasing but by changing the direction of the wave vector of the retrieved light beam. For fixed dark time, one could compensate this, in principle, by changing the alignment of the single-mode fiber.

A fit of the Gaussian model Eq. (4) to the in-trap data in Fig. 4 agrees well with the data. It yields a best-fit value for the  $1/e$  time of  $\tau_F = 12.5(6) \mu\text{s}$ , in good agreement with the prediction  $11.8 \mu\text{s}$  from Eq. (4). In principle, the faster decay of  $\eta$  in the presence of the dipole trap could also be caused by photoionization of the Rydberg state by the trapping light. Quantitatively, however, photoionization is expected to be much slower than the timescale observed here [30].

While release and recapture solves the problem of the reduced in-trap decay time, it causes heating, which drastically reduces the time-averaged data acquisition rate, as discussed above. This limitation could be overcome by operating in blue-detuned or magic-wavelength dipole traps [15,29,31–33]. To obtain a quantitative estimate for the parameters of our experiment, we consider

$$\tau_F = \frac{2\hbar}{mgw_r \left|1 - \frac{\alpha_r}{\alpha_g}\right|} \quad (5)$$

from Eq. (67). Hence, apart from  $w_r$ , the only relevant quantity here is  $|1 - \frac{\alpha_r}{\alpha_g}|$ . For 1064 nm, the above-quoted values of the polarizabilities yield  $|1 - \frac{\alpha_r}{\alpha_g}| = 1.8$ . For 532 nm, however, the polarizabilities are  $\alpha_g = -250$  a.u., see above, and  $\alpha_r = -140$  a.u. estimated from a free electron. This yields  $|1 - \frac{\alpha_r}{\alpha_g}| = 0.45$ . Hence, if we replaced the 1064-nm dipole trap by a 532-nm hollow-beam dipole trap, we would expect an approximately fourfold increase of  $\tau_F$  to  $50 \mu\text{s}$ . Hence,  $\tau_F$  would have a negligible effect compared to the observed  $30 \mu\text{s}$  decay time.

Note that similarly if  $\kappa_g$  is unchanged, then according to Eq. (67)  $\tau_\kappa$  will also improve by a factor of approximately 4 when making the transition to a 532 nm trap, meaning that  $\tau_\kappa$  remains irrelevant.

#### D. Visibility

In addition to the efficiency, the retrieved light has another crucial property, namely the degree to which it is coherent. To quantify this, one can overlap the light with a reference beam, vary the phase of the reference beam, and quote the

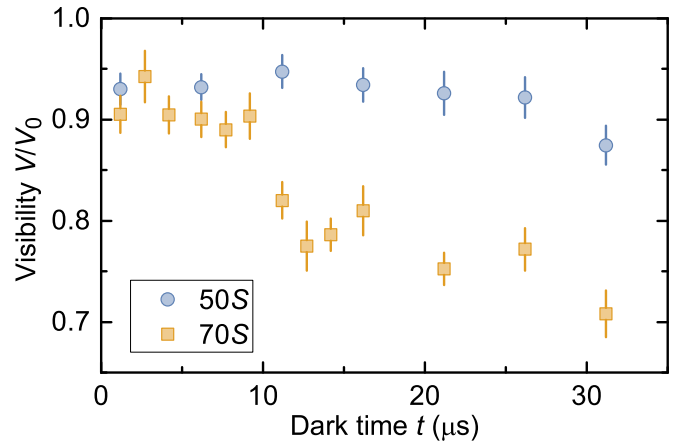


FIG. 5. Dependence of the visibility  $V$  on the dark time  $t$ .  $V$  characterizes how coherent the retrieved light is. It is measured by overlapping the retrieved light with reference light. For short dark time,  $V$  reaches values above 90%. There is a discernible decay as a function of  $t$  for the 70S data, but not for the 50S data. Data are normalized with respect to the technical detection limit  $V_0$  in the present setup. The in-trap peak atomic density is roughly  $2 \times 10^{11} \text{ cm}^{-3}$  for all data in this figure.

fringe visibility  $V = (I_{\max} - I_{\min}) / (I_{\max} + I_{\min})$  of the resulting sinusoidal interference pattern, where  $I_{\max}$  and  $I_{\min}$  denote the maximum and minimum of the intensity. To characterize the coherence of the retrieved light, one will of course quote the value of  $V$  for a parameter setting in which the powers of the two light fields are balanced.

As directed retrieval is a coherent phenomenon,  $\eta$  is also some measure of coherence in the atomic system at the time of retrieval. Hence, one might wonder whether they react identically to experimental imperfections. However, that does not have to be the case. To give an example of a mechanism onto which they react quite differently, we consider shot-to-shot fluctuations of the energy of the Rydberg state. This would cause shot-to-shot fluctuations of the phase of the retrieved light. When taking an ensemble average over many shots, these phase fluctuations would yield a decay of  $V$  as a function of the dark time  $t$ . But the same fluctuations would have no effect whatsoever on  $\eta$ .

In our experiment, we measure  $V$  with a slightly different technique. We overlap the left-hand circularly polarized signal light beam with a copropagating right-hand circularly polarized reference light beam at the same frequency. Polarization tomography reveals the normalized Stokes vector. Here,  $V$  is the length of the projection of the normalized Stokes vector onto the plane which contains all linear polarizations; see, e.g., Ref. [34]. Again, the powers of the signal and reference light must be balanced to avoid underestimating the degree to which the retrieved light is coherent. In the absence of atoms, we measure a visibility of  $V_0 = 97.3(6)\%$ . This is caused, e.g., by imperfections in the polarization tomography, in balancing the beam powers, and in the active stabilization of the differential phase between signal and reference light.  $V_0$  sets the technical detection limit of our present measurement.

Figure 5 shows  $V$  as a function of dark time  $t$  for storage in Rydberg states 50S and 70S after release from the dipole

trap. The values are normalized to the technical detection limit  $V_0$ , which is not related to the physics in the atomic system. The data in Fig. 5 were taken at in-trap peak atomic densities between  $\rho_0 = 1.7 \times 10^{11}$  and  $2.4 \times 10^{11}$  cm $^{-3}$ , temperatures between 0.3 and 0.4  $\mu$ K, and  $L = 0.39$  mm.

The input signal pulse is rectangular and has a duration of 4.5  $\mu$ s out of which only a small fraction near the end of the pulse is stored. This somewhat exaggerated length of the input pulse provides ample time for possible transients to decay. Such transients may result from switching on the pulse. The retrieved pulse has an approximately exponentially decaying shape with a  $1/e$  time of typically 0.8  $\mu$ s, suggesting that the stored part of the input pulse might have had a similar length. As mentioned above, we overlap the left-hand circularly polarized retrieved light with righthand circularly polarized reference light. For simplicity, we use a rectangular pulse shape for the reference light. We process data only in a time interval with a duration of typically 0.5  $\mu$ s, because outside this interval, the beam powers would be poorly balanced.

For short dark time,  $V$  reaches values above 90% in Fig. 5. This is a big improvement over the 66(2)% that we reported in Ref. [16] for a measurement for  $t = 4.5$   $\mu$ s,  $\rho_0 = 2 \times 10^{12}$  cm $^{-3}$ , and storage in state 69S. The much lower atomic density in the present measurement is crucial for this improvement [30].

For storage in the 50S state, we observe no discernible decay of  $V(t)$  in the time interval studied here. Measuring for much longer times would become cumbersome because there would be only a small retrieved signal. For storage in the 70S state, there clearly is a decay of  $V(t)$  but not a very fast one. As the decay depends on the principal quantum number, and as we confirmed in an additional measurement that it does not improve when lowering the atomic density [30], the most likely explanation for the observed decay of  $V(t)$  seems to be a fluctuating Stark shift of the Rydberg state caused by fluctuating stray electric fields.

### III. MODEL

Here, we develop a model for the dark-time decay of the efficiency  $\eta$  in EIT-based storage and retrieval of light. Our model ignores the loss of photons during storage and during the propagation of light inside the medium. Instead, it focuses on the decay of the efficiency as a function of the dark time between storage and retrieval. We start with a brief description of dark polaritons in Sec. III A. This is a straightforward generalization of a similar treatment [3] that did not take photon recoil into account. It sets the stage for the following discussion. In Sec. III B, we use this formalism to derive an expression for the efficiency  $\eta$  for a separable initial state, which may be pure or mixed. The result simplifies if the initial state is uncorrelated, as discussed in Sec. III C. The results can be simplified even further in the frequently encountered situation in which the Hamiltonian for ground-state atoms is identical before and after the storage, as discussed in Sec. III D. The treatment up to that point assumes for simplicity that the mode of the incoming EIT signal field  $u(\mathbf{x})$  is a plane wave. A generalization beyond this assumption is discussed in Sec. III E. The relation to DLCZ sources and to Ramsey spectroscopy is discussed in Sec. III F.

A generalization to entangled initial states is discussed in Appendix C.

#### A. Dark polaritons

We consider EIT-based storage and retrieval in an ensemble of noninteracting, identical, three-level atoms with a ladder-type energy level scheme. A straightforward generalization to  $\Lambda$ -type energy level schemes is discussed in Appendix A. The internal state of an atom has a basis of energy eigenstates that in order of ascending energies are  $|g\rangle$ ,  $|e\rangle$ , and  $|r\rangle$ . In addition, the atom has an external state describing its center-of-mass motion. We assume that a signal (coupling) light field is resonant with the  $|g\rangle \leftrightarrow |e\rangle$  ( $|e\rangle \leftrightarrow |r\rangle$ ) transition; see Fig. 1(b). The coupling light is assumed to be a plane wave  $e^{ik_c \cdot x}$  with wave vector  $\mathbf{k}_c$ . We consider only a single mode of the EIT signal light with mode function  $u(\mathbf{x})$  normalized to  $\int_{\mathcal{V}} d^3x |u(\mathbf{x})|^2 = 1$ , where  $\mathcal{V}$  is the quantization volume. We abbreviate  $v(\mathbf{x}) = u(\mathbf{x})e^{ik_c \cdot x}$ . This is normalized to  $\int_{\mathcal{V}} d^3x |v(\mathbf{x})|^2 = 1$ . For simplicity, the following description assumes that  $u(\mathbf{x})$  is a plane wave  $u(\mathbf{x}) = e^{i\mathbf{k}_s \cdot \mathbf{x}} / \sqrt{\mathcal{V}}$  with wave vector  $\mathbf{k}_s$ . A generalization beyond this assumption is discussed in Sec. III E.  $\hbar\mathbf{k}_R$  with  $\mathbf{k}_R = \mathbf{k}_s + \mathbf{k}_c$  is the recoil momentum transferred to an atom in the two-photon transition from  $|g\rangle$  to  $|r\rangle$ .

While the initial state  $|g\rangle$  and final state  $|r\rangle$  of the storage process are assumed to be long-lived, the intermediate state  $|e\rangle$  is subject to decay to state  $|g\rangle$  with a rate coefficient  $\Gamma_e$  accompanied by emission of a photon. The desired part of these emissions produces photons in mode  $u(\mathbf{x})$ . The remaining part produces photons in spatial modes orthogonal to  $u(\mathbf{x})$ . We refer to the latter process as spontaneous emission.

We define the number of excitations as the number of signal photons in mode  $u(\mathbf{x})$  plus the number of atoms in states  $|e\rangle$  and  $|r\rangle$ . In the absence of spontaneous emission, the number of excitations is conserved. As a result, the subspaces of Hilbert space describing states with a given number of excitations are invariant under time evolution as long as spontaneous emission is ignored. In the presence of spontaneous emission, the number of excitations can only decrease. In our experiment, the number of stored excitations is typically less than one. Hence, we restrict our model to the subspaces with one or zero excitations. The zero-excitation subspace is trivial, so we focus on the single-excitation subspace.

Hence, EIT-based storage starts with one photon in mode  $u(\mathbf{x})$  and all atoms in internal state  $|g\rangle$ . The external initial state, however, is often a mixed state. The initial  $N$ -atom state can generally be described by a density matrix  $\rho_{N,\text{in}}$ , where the subscript ‘‘in’’ indicates the initial state before storage. For simplicity, we restrict the discussion here to situations in which  $\rho_{N,\text{in}}$  is separable. The model is easily extended to entangled initial states, see Appendix C. As the density matrix  $\rho_{N,\text{in}}$  is separable, it can be written as (see, e.g., Ref. [35])

$$\rho_{N,\text{in}} = \sum_n P_n |\Psi_{g,n,\text{in}}\rangle \langle \Psi_{g,n,\text{in}}|, \quad (6)$$

where each of the initial  $N$ -atom pure states  $|\Psi_{g,n,\text{in}}\rangle$  is separable, i.e., a product of  $N$  single-atom states. The probabilities  $P_n$  fulfill  $P_n \geq 0$  and  $\sum_n P_n = 1$ . Obviously, the storage-and-retrieval efficiency for the initial state  $\rho_{N,\text{in}}$  of

Eq. (6) is

$$\eta(t) = \sum_n P_n \eta_n(t), \quad (7)$$

where  $t$  is the dark time and  $\eta_n(t)$  denotes the storage-and-retrieval efficiency that would be obtained if the initial state was the pure state  $|\Psi_{g,n,\text{in}}\rangle$ .

To calculate  $\eta_n(t)$  we note that, as stated above, the pure state  $|\Psi_{g,n,\text{in}}\rangle$  is assumed to be a product state with all atoms in internal state  $|g\rangle$ . Hence, it has the form  $|\Psi_{g,n,\text{in}}\rangle = \bigotimes_{i=1}^N |\psi_{g,n,i}(0), g_i\rangle$ , where  $|\psi_{g,n,i}(0)\rangle$  and  $|g_i\rangle$  are the initial external and internal states of the  $i$ th atom, respectively. The argument (0) in  $|\psi_{g,n,i}(0)\rangle$  refers to zero dark time. Throughout this paper,  $N$ -atom states (external single-atom states) are represented by uppercase Greek letters (lowercase Greek letters).

It is easy to show that the three-dimensional (3D) subspace of Hilbert space spanned by the orthonormal set of  $N$ -atom states,

$$|\Psi_{g,n,\text{in}}, 1_s\rangle = |1_s\rangle \bigotimes_{i=1}^N |\psi_{g,n,i}(0), g_i\rangle, \quad (8a)$$

$$|\Psi_{e,n}(0)\rangle = \frac{1}{\sqrt{N}} \sum_{i=1}^N |\psi_{e,n,i}(0), e_i\rangle \bigotimes_{\substack{i'=1 \\ i' \neq i}}^N |\psi_{g,n,i'}(0), g_{i'}\rangle, \quad (8b)$$

$$|\Psi_{r,n}(0)\rangle = \frac{1}{\sqrt{N}} \sum_{i=1}^N |\psi_{r,n,i}(0), r_i\rangle \bigotimes_{\substack{i'=1 \\ i' \neq i}}^N |\psi_{g,n,i'}(0), g_{i'}\rangle, \quad (8c)$$

is invariant under application of the atom-light interaction Hamiltonian  $\mathcal{V}_{\text{al}}$  detailed in Appendix A. Here,  $|1_s\rangle$  is the single-photon Fock state of the mode  $u(\mathbf{x})$  of the signal light. The external single-atom states  $|\psi_{e,n,i}(0)\rangle$  and  $|\psi_{r,n,i}(0)\rangle$  have the position representations

$$\psi_{e,n,i}(\mathbf{x}, 0) = \sqrt{V} u(\mathbf{x}) \psi_{g,n,i}(\mathbf{x}, 0), \quad (9a)$$

$$\psi_{r,n,i}(\mathbf{x}, 0) = \sqrt{V} v(\mathbf{x}) \psi_{g,n,i}(\mathbf{x}, 0) \quad (9b)$$

and are properly normalized because  $u(\mathbf{x})$  and  $v(\mathbf{x})$  are properly normalized plane waves. The  $N$ -atom states  $|\Psi_{e,n}(0)\rangle$  and  $|\Psi_{r,n}(0)\rangle$  are singly excited Dicke states, in which we omitted multiplication with the vacuum state  $|0_s\rangle$  of the signal mode for brevity.

For later use, we introduce an operator  $R_i^\dagger$  acting on the external degree of the  $i$ th atom with position representation

$$R_i^\dagger(\mathbf{x}) = \sqrt{V} v(\mathbf{x}). \quad (10)$$

Hence Eq. (9b) can be rewritten as

$$|\psi_{r,n,i}(0)\rangle = R_i^\dagger |\psi_{g,n,i}(0)\rangle. \quad (11)$$

As  $v(\mathbf{x})$  is a plane wave,  $R_i^\dagger$  is unitary. A related single-particle operator  $S_{r,i}^\dagger = R_i^\dagger \otimes |r_i\rangle\langle g_i|$  acting on the external and internal degrees of freedom of the  $i$ th atom is studied in Ref. [30].

It is easy to show that with respect to the orthonormal basis  $[|\Psi_{g,n,\text{in}}, 1_s\rangle, |\Psi_{e,n}(0)\rangle, |\Psi_{r,n}(0)\rangle]$  of the 3D invariant subspace, the atom-light interaction Hamiltonian  $\mathcal{V}_{\text{al}}$  has the

matrix representation

$$\mathcal{V}_{\text{al}} = \frac{\hbar}{2} \begin{pmatrix} 0 & 2g_R\sqrt{N} & 0 \\ 2g_R\sqrt{N} & 0 & \Omega_c \\ 0 & \Omega_c & 0 \end{pmatrix}, \quad (12)$$

where  $2g_R$  is the vacuum Rabi frequency of the signal mode and  $\Omega_c$  is the Rabi frequency of the EIT coupling light. The factor  $\sqrt{N}$  comes about because  $g_R$  causes transitions between a product state and a Dicke state.

Obviously, the  $N$ -atom state

$$|\Psi_{d,n}(\vartheta)\rangle = \cos \vartheta |\Psi_{g,n,\text{in}}, 1_s\rangle - \sin \vartheta |\Psi_{r,n}(0)\rangle \quad (13)$$

with mixing angle  $\vartheta$  given by

$$\tan \vartheta = \frac{2g_R\sqrt{N}}{\Omega_c} \quad (14)$$

is an eigenstate of  $\mathcal{V}_{\text{al}}$ . Hence, for signal light in vacuum with  $\Omega_c \neq 0$ , one obtains  $\vartheta = 0$ . If we were to extend our formalism to a signal light pulse instead of a plane wave, then  $\vartheta = 0$  would be the initial value before the pulse enters the medium and the final value after the retrieved pulse left the medium. Conversely, for a pulse inside the medium with  $\Omega_c = 0$  during the dark time between storage and retrieval, one would obtain  $\vartheta = \pi/2$ .

The state  $|\Psi_{d,n}\rangle$  is dark in the sense that it shows no spontaneous emission when spontaneous emission into modes orthogonal to  $u(\mathbf{x})$  is added to the model, because  $\langle e_i | \Psi_{d,n} \rangle = 0$  for all  $i$ . For  $0 < \vartheta < \pi/2$ , the state  $|\Psi_{d,n}\rangle$  describes a superposition of a photon and a copropagating atomic excitation, which is why it is called a dark polariton. For  $\vartheta = 0$ , however, it describes a single photon and for  $\vartheta = \pi/2$  it describes the Dicke state  $|\Psi_{r,n}(0)\rangle$ , which is commonly referred to as a spin wave.

The other two eigenstates of  $\mathcal{V}_{\text{al}}$  in Eq. (12) are bright states because they rapidly decay by spontaneous emission into modes orthogonal to  $u(\mathbf{x})$ . In our model, these bright states that couple to  $u(\mathbf{x})$  never become populated because we will assume below that the population adiabatically follows the dark state  $|\Psi_{d,n}\rangle$ .

## B. EIT-based storage and retrieval

In an experiment, a signal light pulse of finite duration is stored in an atomic medium of finite length. Aiming at large storage efficiency would entail a nontrivial treatment of the longitudinal wave function of the signal light pulse, particularly when entering and leaving the medium. In addition, one would need to address the question of whether the complete light pulse fits into the medium longitudinally. If that is not the case, this will lead to leakage of signal light through the medium during the time of storage. Furthermore, there is the issue of residual absorption because of imperfect EIT while the pulse propagates inside the medium before storage and after retrieval. The residual absorption can be caused, e.g., by dephasing or by the nonzero frequency width of the light pulse which results from its finite duration. Such issues have been addressed in the literature in detail; see, e.g., Ref. [36]. We do not attempt to model leakage and residual absorption here because these issues tend to affect the efficiency in a way that is independent of the dark time. In Eq. (18), leakage



and residual absorption will be subsumed in an empirical correction factor  $\eta_0$ .

To describe storage, we use a model quite similar to Refs. [2,3]. In this model, the medium is homogeneous along the  $z$  axis with a quantization length  $L_z$ . Hence, the signal-light pulse cannot enter or leave the medium and no spatial pulse compression occurs, which drastically simplifies the model. The experimental initial situation with a light pulse outside the medium is modeled by starting with a very large value of  $\Omega_c$ , which results in  $\vartheta \approx 0$ . Along with this, the system is assumed to be prepared in the dark state  $|\Psi_{d,n}\rangle = |\Psi_{g,n,\text{in}}, 1_s\rangle$ . Next,  $\Omega_c$  is ramped to 0. We assume that this ramp is slow enough that the population, to a good approximation, adiabatically follows the dark state. The time evolution during the ramp, which can be fairly complicated in general, is thus simply modeled as adiabatic following, much like in Ref. [3]. After this ramp,  $\vartheta = \pi/2$  so that the dark state has evolved into  $|\Psi_{d,n}\rangle = |\Psi_{r,n}(0)\rangle$ , which means that storage in the form of a spin wave has been achieved. The assumption of adiabatic following means that no spontaneous emission into modes orthogonal to  $u(\mathbf{x})$  occurs during storage.

As an aside, we note that in an experiment, the rotation of  $\vartheta$  occurs almost exclusively when the pulse enters the medium. When the pulse is inside the homogeneous part of the medium, typically  $\vartheta \approx \pi/2$ . The actual temporal ramp of  $\Omega_c$  in the experiment changes  $\vartheta$  only by a small amount, bringing it all the way to  $\pi/2$ .

Now, we deviate from Refs. [2,3]. We further simplify the model by assuming that  $u(\mathbf{x})$  is a plane wave. As a result, keeping track of the longitudinal properties of the signal light becomes trivial.

We now turn to the dark time  $t$  between storage and retrieval. As the Hamiltonian is time-independent during the dark time, it yields a time-evolution operator of the simple form  $\mathcal{U}_d(t) = e^{-i\mathcal{H}_d t/\hbar}$ , where  $\mathcal{H}_d$  is the  $N$ -atom dark-time Hamiltonian. For simplicity, we restrict our model to a situation in which  $\mathcal{H}_d = \sum_{i=1}^N H_{d,i}$  is a sum of single-atom Hamiltonians  $H_{d,i}$  of the form

$$H_{d,i} = H_{g,i} \otimes |g_i\rangle\langle g_i| + H_{r,i} \otimes |r_i\rangle\langle r_i|, \quad (15)$$

where  $H_{g,i}$  and  $H_{r,i}$  are operators acting on the external state of the  $i$ th atom. Hence, the atoms are noninteracting and the internal state of each atom is unchanged during the dark time. We abbreviate

$$U_{g,i}(t) = e^{-iH_{g,i}t/\hbar}, \quad |\psi_{g,n,i}(t)\rangle = U_{g,i}|\psi_{g,n,i}(0)\rangle, \quad (16a)$$

$$U_{r,i}(t) = e^{-iH_{r,i}t/\hbar}, \quad |\psi_{r,n,i}(t)\rangle = U_{r,i}|\psi_{r,n,i}(0)\rangle. \quad (16b)$$

Throughout this paper,  $N$ -atom (single-atom) operators other than the density matrix are represented by uppercase calligraphic (italic) letters.

Hence, the  $N$ -atom state at the end of the dark time reads

$$\begin{aligned} |\Psi_{r,n}(t)\rangle &= \mathcal{U}_d(t)|\Psi_{r,n}(0)\rangle \\ &= \frac{1}{\sqrt{N}} \sum_{i=1}^N |\psi_{r,n,i}(t), r_i\rangle \bigotimes_{\substack{i'=1 \\ i' \neq i}}^N |\psi_{g,n,i'}(t), g_{i'}\rangle. \end{aligned} \quad (17)$$

Typically, the term  $\mathcal{H}_d$  in the Hamiltonian will also be present during storage and retrieval. But for simplicity, we assume

that the dynamics during storage and retrieval are dominated by  $\mathcal{V}_{\text{al}}$  so that  $\mathcal{H}_d$  has a negligible effect during storage and retrieval.

After the dark time, the EIT coupling light is turned back on for retrieval. Ideally, this will cause directed retrieval of the photon into the original spatial mode  $u(\mathbf{x})$  as a result of interference of light emitted from the large number  $N$  of atoms [2,3]. The write-read efficiency  $\eta$  is the ratio of the average number of photons retrieved into the original mode  $u(\mathbf{x})$  divided by the average number of incoming photons before storage. Again, we neglect a variety of experimental complications, e.g., the fact that after the finite-duration signal light pulse resumes propagation, it experiences some residual absorption before leaving the finite-length medium. Instead, we model the retrieval process by assuming that  $\Omega_c$  is slowly ramped back up from zero, where  $\vartheta = \pi/2$ , to a very large value of  $\Omega_c$ , finally resulting in  $\vartheta \approx 0$ . We study the final number of photons in the plane-wave mode  $u(\mathbf{x})$ , which remains inside the homogeneous medium and does not experience absorption in our model because it is monochromatic and meets the two-photon resonance condition.

Hence, much like the storage process, we model the retrieval as an adiabatic passage, but now with  $\vartheta$  evolving back from  $\pi/2$  to 0. For zero dark time, the considerations can be restricted to the 3D invariant subspace given by Eq. (8), and the retrieval is simply the time-reversed process of the storage. For nonzero dark time, however, things become more complicated. If retrieval is successful, then by definition the excitation reappears in the mode  $u(\mathbf{x})$  of the signal light, which obviously implies that all atoms are finally in internal state  $|g\rangle$ . But for nonzero dark time it is not immediately clear what the final external  $N$ -atom state will be.

To include this aspect in our calculation, let  $\mathcal{H}_{\text{ext}}$  denote the Hilbert space containing all external  $N$ -atom states. Note that the fact that  $\mathcal{H}_{\text{ext}}$  is a Hilbert space implies that it contains product states and entangled states. Let  $W_u$  denote the subspace of spin-wave states obtained when applying storage with mode function  $u(\mathbf{x})$  to  $\mathcal{H}_{\text{ext}}$ . Let us temporarily assume that the state after the dark time  $|\Psi_{r,n}(t)\rangle$  is an element of  $W_u$ . Hence, there exists an  $N$ -atom state  $|\Psi_f\rangle$  that would turn into  $|\Psi_{r,n}(t)\rangle$  upon storage. As we treat the retrieval as the time-reversed version of storage, it is now clear that the state  $|\Psi_{r,n}(t)\rangle$  causes retrieval with 100% efficiency into mode  $u(\mathbf{x})$  with final atomic state  $|\Psi_f\rangle$ . In this way, we found the possibly nontrivial final  $N$ -atom state  $|\Psi_f\rangle$ .

Now we turn to a general state  $|\Psi_{r,n}(t)\rangle$ , which does not have to be an element of  $W_u$ . We use  $\mathcal{P}_u$  to denote the orthogonal projector onto the subspace  $W_u$  and use this to decompose this state into  $\mathcal{P}_u|\Psi_{r,n}(t)\rangle$  and  $(\mathbb{1} - \mathcal{P}_u)|\Psi_{r,n}(t)\rangle$ . As  $\mathcal{P}_u|\Psi_{r,n}(t)\rangle$  is an element of  $W_u$ , it causes retrieval into mode  $u(\mathbf{x})$  with perfect efficiency, as explained above. Conversely, as  $(\mathbb{1} - \mathcal{P}_u)|\Psi_{r,n}(t)\rangle$  is orthogonal to  $W_u$  it does not couple to the mode  $u(\mathbf{x})$  for reasons discussed in Appendix B. Hence, the efficiency is

$$\eta_n(t) = \eta_0 \|\mathcal{P}_u|\Psi_{r,n}(t)\rangle\|^2, \quad (18)$$

where  $\|\dots\|$  denotes the norm of a vector and we included a constant factor  $\eta_0$  with  $0 \leq \eta_0 \leq 1$ , which serves to represent imperfections during storage and retrieval, such as leakage, residual absorption, and imperfections in the adiabaticity

when rotating  $\vartheta$ . We assume that  $\eta_0$  is independent of  $n$ . In the following we always consider  $N \gg 1$ , because this is a necessary condition for making the directed emission dominate over spontaneous emission in random directions.

As detailed in Appendix B, Eq. (18) with  $N \gg 1$  yields for a separable pure initial state

$$\frac{\eta_n(t)}{\eta_0} = \frac{1}{N^2} \left| \sum_{i=1}^N Q_{n,i}(t) \right|^2 \quad (19)$$

with

$$\begin{aligned} Q_{n,i}(t) &= \langle \psi_{g,n,i}(t) | R_i | \psi_{r,n,i}(t) \rangle \\ &= \langle \psi_{g,n,i}(0) | U_{g,i}^\dagger(t) R_i U_{r,i}(t) R_i^\dagger | \psi_{g,n,i}(0) \rangle. \end{aligned} \quad (20)$$

Note that Eq. (11) combined with  $\langle \psi_{r,n,i}(0) | \psi_{r,n,i}(0) \rangle = 1$  implies  $Q_{n,i}(0) = 1$  so that  $\eta_n(0)/\eta_0 = 1$ . In addition, the unitarity of  $R_i$  implies  $|Q_{n,i}(t)|^2 \leq 1$  for all times so that  $\eta_n(t)/\eta_0 \leq 1$  for all times.

Equation (19) for a separable pure initial state can equivalently be written as

$$\frac{\eta_n(t)}{\eta_0} = |\langle \Phi_n(t) | \Psi_{r,n}(t) \rangle|^2 \quad (21)$$

with a properly normalized Dicke state

$$|\Phi_n(t)\rangle = \frac{1}{\sqrt{N}} \sum_{i=1}^N (R_i^\dagger | \psi_{g,n,i}(t), r_i \rangle) \bigotimes_{\substack{i'=1 \\ i' \neq i}}^N | \psi_{g,n,i'}(t), g_{i'} \rangle, \quad (22)$$

which turns out to be an element of  $W_u$ . In the language of quantum information processing,  $\eta_n(t)/\eta_0$  in Eq. (21) is the fidelity [37] of the states  $|\Phi_n(t)\rangle$  and  $|\Psi_{r,n}(t)\rangle$ .

The  $N$ -atom state  $|\Psi_{r,n}(t)\rangle$  is obtained from the state  $|\Psi_{g,n,\text{in}}, 1_s\rangle$  by storage followed by dark-time propagation, whereas the  $N$ -atom state  $|\Phi_n(t)\rangle$  would be obtained if the temporal order were reversed, namely if the dark-time propagation were followed by storage. Equation (20) features analogous quantities on the single-particle level, because  $|\psi_{r,n,i}(t)\rangle$  is obtained from  $|\psi_{g,n,i}(0)\rangle$  by storage followed by dark-time propagation, whereas  $R_i^\dagger | \psi_{g,n,i}(t) \rangle$  would be obtained by dark-time propagation followed by storage.

Equation (19) is immediately applicable to a gas of noninteracting bosons at  $T = 0$ , because in that case one obtains a pure BEC so that all atoms initially occupy the same single-particle wave function. In this situation, we drop the indices  $n, i$  from the notation and obtain

$$\frac{\eta_{\text{BEC}}(t)}{\eta_0} = |Q(t)|^2. \quad (23)$$

More generally, inserting Eq. (19) into Eq. (7), one immediately finds  $\eta(t)$  for the arbitrary separable initial state of Eq. (6), which may be mixed.

### C. Uncorrelated initial state

We now concentrate on a special case, which is experimentally relevant and allows for further simplifications, finally giving a simple expression. Specifically, we assume that the

initial  $N$ -atom density matrix

$$\rho_{N,\text{in}} = \underbrace{\tilde{\rho}_{\text{in}} \otimes \tilde{\rho}_{\text{in}} \otimes \cdots \otimes \tilde{\rho}_{\text{in}}}_{N \text{ times}} \quad (24)$$

is a tensor product of  $N$  identical copies of a single-atom density matrix  $\tilde{\rho}_{\text{in}}$ . As all atoms are initially in internal state  $|g\rangle$ , we obtain  $\tilde{\rho}_{\text{in}} = \rho_{\text{in}} \otimes |g\rangle\langle g|$ , where  $\rho_{\text{in}}$  describes only the external state of a single atom. Note that  $\rho_{\text{in}}$  can be diagonalized as

$$\rho_{\text{in}} = \sum_n p_n | \psi_{g,n}(0) \rangle \langle \psi_{g,n}(0) | \quad (25)$$

with probabilities  $p_n$ . Inserting this into Eq. (24) shows that  $\rho_{N,\text{in}}$  is separable so that the above formalism is applicable.

As we assumed that the particles are identical, Eq. (24) holds if and only if all particles are uncorrelated, which is the case, e.g., if  $\rho_{N,\text{in}}$  describes a noninteracting gas of identical particles in thermal equilibrium at a temperature far above quantum degeneracy. In that case,  $p_n$  is given by Eq. (46) and the external single-atom states  $| \psi_{g,n}(0) \rangle$  are the eigenstates of the Hamiltonian before storage. Note that a noninteracting pure BEC at  $T = 0$  is also an example of the uncorrelated initial state in Eq. (24). In that case,  $\rho_{\text{in}}$  is a pure state.

In addition, as we assumed that the particles are identical, we obtain  $H_{g,i} = H_{g,1}$  and  $H_{r,i} = H_{r,1}$  for all  $i$ . As a result, the problem factorizes and all properties of the  $N$ -atom problem can be expressed in terms of properties of only the first particle. In this situation, we drop the index  $i$  from the notation, writing, e.g.,  $H_g = H_{g,1}$  and  $Q_n(t) = Q_{n,1}(t)$ .

The fact that all properties of the  $N$ -atom problem can be expressed in terms of the properties of only the first particle drastically simplifies the problem. A straightforward calculation based on Eq. (19) yields for an uncorrelated initial state and  $N \gg 1$

$$\frac{\eta(t)}{\eta_0} = |C(t)|^2 \quad (26)$$

with

$$C(t) = \sum_n p_n Q_n(t). \quad (27)$$

This is a complex number, which we call the coherence. Note that  $Q_n(0) = 1$  for all  $n$  implies

$$C(0) = 1 \quad (28)$$

as long as  $u(\mathbf{x})$  is a plane wave. Inserting  $Q_n(t)$  from Eq. (20) yields

$$\begin{aligned} C(t) &= \sum_n p_n \langle \psi_{g,n}(0) | U_g^\dagger(t) R U_r(t) R^\dagger | \psi_{g,n}(0) \rangle \\ &= \text{tr}[\rho_{\text{in}} U_g^\dagger(t) R U_r(t) R^\dagger]. \end{aligned} \quad (29)$$

Before proceeding, we note for later use that if

$$R = \mathbb{1} \quad \text{and} \quad H_g = H_r, \quad (30)$$

then Eq. (20) obviously yields  $Q_n(t) = 1$  for all  $n, t$  and we obtain  $\eta(t)/\eta_0 = 1$  for all  $t$ .

In addition, we note for later use that there are a number of situations in which the problem separates in Cartesian coordinates. Specifically, if the time-evolution operator fulfills

$U_g(\mathbf{p}, \mathbf{x}) = U_{g,x}(p_x, x)U_{g,y}(p_y, y)U_{g,z}(p_z, z)$  and if an analogous statement holds for  $U_r(\mathbf{p}, \mathbf{x})$ ,  $v(\mathbf{x})$ , and  $\psi_{g,n}(\mathbf{x}, 0)$  for all  $n$  and if the probabilities fulfill  $p_n = p_{n_x}p_{n_y}p_{n_z}$  for all  $n$ , then according to Eq. (20)  $Q_{n,i}(t) = Q_{n_x,x}(t)Q_{n_y,y}(t)Q_{n_z,z}(t)$  and according to Eqs. (26) and (27)

$$\frac{\eta(t)}{\eta_0} = \frac{\eta_x(t)}{\eta_{x,0}} \frac{\eta_y(t)}{\eta_{y,0}} \frac{\eta_z(t)}{\eta_{z,0}}. \quad (31)$$

#### D. Same ground-state Hamiltonian before and during the dark time

To further simplify the model, we assume that the initial  $N$ -atom density matrix  $\rho_{N,\text{in}}$  commutes with the dark-time Hamiltonian  $\mathcal{H}_g = \sum_{i=1}^N H_{g,i}$  for  $N$  atoms in internal state  $|g\rangle$ ,

$$[\mathcal{H}_g, \rho_{N,\text{in}}] = 0. \quad (32)$$

This equation holds, e.g., in the frequently encountered situation in which  $\rho_{N,\text{in}}$  is in thermal equilibrium before storage and the ground-state Hamiltonian  $\mathcal{H}_g$  is identical before storage and during the dark time.

Equation (32) implies that all the  $|\psi_{g,n,i}(0)\rangle$  can be chosen such that they are eigenstates of  $H_{g,i}$ . Let the corresponding eigenvalues be denoted as  $E_{g,n,i}$ . This yields

$$|\psi_{g,n,i}(t)\rangle = e^{-iE_{g,n,i}t/\hbar} |\psi_{g,n,i}(0)\rangle \quad (33)$$

so that using Eq. (10), we find that Eq. (20) simplifies to

$$Q_{n,i}(t) = e^{iE_{g,n,i}t/\hbar} \langle \psi_{r,n,i}(0) | \psi_{r,n,i}(t) \rangle. \quad (34)$$

The corresponding Eq. (21) for  $N$ -atom states simplifies to

$$\frac{\eta_n(t)}{\eta_0} = |\langle \Psi_{r,n}(0) | \Psi_{r,n}(t) \rangle|^2. \quad (35)$$

The last equation has been used previously, e.g., in Refs. [13,14,22] without much justification.

A particularly simple example is obtained if additionally the  $|\psi_{r,n,i}(0)\rangle$  for all  $n$  are eigenstates of the dark-time Hamiltonian  $H_{r,i}$  with eigenvalues  $E_{r,n,i}$ . This yields

$$|\psi_{r,n,i}(t)\rangle = e^{-iE_{r,n,i}t/\hbar} |\psi_{r,n,i}(0)\rangle \quad (36)$$

so that Eq. (34) simplifies to

$$Q_{n,i}(t) = e^{i(E_{g,n,i} - E_{r,n,i})t/\hbar} \langle \psi_{r,n,i}(0) | \psi_{r,n,i}(0) \rangle. \quad (37)$$

As long as  $u(\mathbf{x})$  is a plane wave,  $\langle \psi_{r,n,i}(0) | \psi_{r,n,i}(0) \rangle = 1$ , as discussed above.

#### E. Beyond a plane-wave signal light field

The formalism discussed so far can be extended to situations in which the mode function  $u(\mathbf{x})$  of the signal light is not a plane wave, as detailed in Appendix D. Here, we briefly summarize the central results of that treatment. This treatment is experimentally relevant because typically  $w_r \approx w$ , as pointed out in the context of Eq. (3). Hence, the finite signal beam waist  $w$  is crucial for correctly modeling the radius  $w_r$  of the part of the atom cloud that was transferred into state  $|r\rangle$  during storage.

The quantities  $|\psi_{g,n,i}(t)\rangle$ ,  $|\psi_{r,n,i}(t)\rangle$ ,  $R_i^\dagger$ ,  $Q_{n,i}(t)$ , and  $C(t)$  are still defined by Eqs. (9), (10), (16), (20), and (27). In addition to imprinting the phase factor that represents the net photon recoil, the operator  $R_i^\dagger$  now also imprints the

finite beam waist  $w$  onto the part of the atom cloud that was transferred into state  $|r\rangle$  during storage. But now the operator  $R_i^\dagger$  is no longer unitary and the single-particle state  $R_i^\dagger |\psi_{g,n,i}(t)\rangle$  that appears in the definition (20) of  $Q_{n,i}(t)$  is no longer properly normalized. Instead, calculating its norm squared yields a dimensionless real number

$$\begin{aligned} M_{n,i}(t) &= \langle \psi_{g,n,i}(t) | R_i^\dagger R_i | \psi_{g,n,i}(t) \rangle \\ &= \mathcal{V} \int_{\mathcal{V}} d^3x |u(\mathbf{x}) \psi_{g,n,i}(\mathbf{x}, t)|^2, \end{aligned} \quad (38)$$

which describes how well the mode  $u(\mathbf{x})$  overlaps with the atomic wave function  $\psi_{g,n,i}(\mathbf{x}, t)$ . Note that combination with Eq. (11) yields  $\langle \psi_{r,n,i}(0) | \psi_{r,n,i}(0) \rangle = M_{n,i}(0)$ .

As shown in Appendix D, Eq. (23) generalizes to

$$\frac{\eta_{\text{BEC}}(t)}{\eta_0} = \frac{|Q(t)|^2}{M(0)M(t)}. \quad (39)$$

We turn to the uncorrelated state of Eq. (24). As shown in Appendix D, Eq. (26) generalizes to

$$\frac{\eta(t)}{\eta_0} = \frac{|C(t)|^2}{\mu(0)\mu(t)}, \quad (40)$$

where

$$\mu(t) = \sum_n p_n M_n(t) = \mathcal{V} \int_{\mathcal{V}} d^3x |u(\mathbf{x})|^2 \varrho_g(\mathbf{x}, t) \quad (41)$$

is the average of all the  $M_n(t)$  and

$$\varrho_g(\mathbf{x}, t) = \sum_n p_n |\psi_{g,n}(\mathbf{x}, t)|^2 \quad (42)$$

is the spatial density distribution of a single atom, normalized to  $\int_{\mathcal{V}} d^3x \varrho_g(\mathbf{x}, t) = 1$ . Note that  $\mu(0) = C(0)$  according to Appendix D.

If Eq. (32) holds, typically because the Hamiltonian is identical before and after storage, then according to Appendix D we obtain  $\mu(t) = \mu(0)$  so that Eq. (40) simplifies to

$$\frac{\eta(t)}{\eta_0} = \left| \frac{C(t)}{C(0)} \right|^2 \quad (43)$$

and Eqs. (34) and (37) remain unchanged, now with  $\langle \psi_{r,n}(0) | \psi_{r,n}(0) \rangle = M_n(0)$  according to the text below Eq. (38).

#### F. Relation to DLCZ sources and Ramsey spectroscopy

The central results of Secs. III B–III E also apply to single-photon sources based on the DLCZ protocol [20]. This is because the write pulse of a DLCZ source, while using a somewhat different mechanism, prepares the Dicke state  $|\Psi_{r,n}(0)\rangle$  of Eq. (8c). The subsequent time evolution during the dark time and during the DLCZ read pulse is largely identical to the dark time and the retrieval in EIT-based storage and retrieval. Hence, processes that cause the efficiency to decay as a function of dark time affect DLCZ sources and EIT-based storage and retrieval in the same way.

Furthermore, as shown in Ref. [30], an appropriately designed Ramsey experiment with the purely kinetic dark-time

Hamiltonian of Eq. (47) has fringe visibility

$$V(t) = \left| \frac{C_1(t)}{C_1(0)} \right| \quad (44)$$

with  $C_1(t)$  defined in Ref. [30]. This equation holds for a plane-wave signal beam  $u(\mathbf{x})$  and an arbitrary initial state. Alternatively, it also holds if the pulse area of the Ramsey pulses is small and  $\rho_{N,\text{in}}$  commutes with the dark-time Hamiltonian. For an uncorrelated initial state or for Ramsey spectroscopy performed on a single atom,  $C_1(t)$  becomes identical to  $C(t)$  from Eq. (29).

For an uncorrelated initial state with a plane-wave signal beam, Eqs. (26) and (28) hold and combination with Eq. (44) and  $C_1(t) = C(t)$  yields

$$\frac{\eta(t)}{\eta_0} = V^2(t). \quad (45)$$

Alternatively, if the initial state is uncorrelated, and  $\rho_{N,\text{in}}$  commutes with the dark-time Hamiltonian, then Eq. (43) holds and combination with Eq. (44) and  $C_1(t) = C(t)$  yields Eq. (45). Hence, in both of these situations, the analysis of the processes that cause the visibility in Ramsey spectroscopy and the efficiency in EIT-based storage and retrieval to decay as a function of dark time are equivalent. Studying whether this equivalence holds for other initial states is beyond the present scope.

#### IV. APPLICATIONS OF THE MODEL

In this section, we apply the above model to a few selected situations. The first situation, discussed in Sec. IV A, deals with the decay of  $\eta$  caused by photon recoil during storage combined with thermal atomic motion. This situation is closely related to the spatial first-order coherence function of the gas, as pointed out in Sec. IV B. In Sec. IV C, we use the Raman-Nath approximation to derive an expression for the decay of  $\eta$  resulting if atoms in states  $|g\rangle$  and  $|r\rangle$  experience different potentials  $V_g(\mathbf{x})$  and  $V_r(\mathbf{x})$  during the dark time. In Sec. IV D, we apply this expression to a situation in which both  $V_g(\mathbf{x})$  and  $V_r(\mathbf{x})$  are harmonic, and gravitational sag is taken into account.

##### A. Photon recoil and thermal motion

Here we discuss the decay of  $\eta$  caused by nonzero total photon recoil  $\hbar\mathbf{k}_R$  during storage combined with thermal atomic motion at a temperature  $T$  far above quantum degeneracy. For simplicity, we assume that the EIT signal light mode  $u(\mathbf{x})$  is a plane wave. According to Eq. (27), we only need to consider single-particle properties. The  $|\psi_{g,n}(0)\rangle$  are the eigenstates of the Hamiltonian  $H_g$  before storage. The probability of occupying the  $n$ th single-particle state is

$$p_n = \frac{1}{Z} e^{-\beta E_{g,n}}, \quad (46)$$

where the normalization constant  $Z = \sum_n e^{-\beta E_{g,n}}$  is the canonical partition function and  $\beta = 1/k_B T$ .

We assume that the single-atom Hamiltonian before and after storage is

$$H_g = H_r = \frac{\mathbf{p}^2}{2m}, \quad (47)$$

where  $\mathbf{p}$  and  $m$  are the momentum and the mass of the atom, i.e., the single-particle potentials vanish before and after storage,  $V_g(\mathbf{x}) = V_r(\mathbf{x}) = 0$ . Hence, the  $|\psi_{g,n}(0)\rangle$  have the position representation

$$\psi_{g,n}(\mathbf{x}, 0) = \frac{e^{i\mathbf{k}_n \cdot \mathbf{x}}}{\sqrt{\mathcal{V}}} \quad (48)$$

with wave vectors  $\mathbf{k}_n$  meeting periodic boundary conditions. The external states  $\psi_{r,n}(\mathbf{x}, 0) = e^{i(\mathbf{k}_n + \mathbf{k}_R) \cdot \mathbf{x}} / \sqrt{\mathcal{V}}$  created during storage are eigenstates of the dark-time Hamiltonian so that Eqs. (27) and (37) apply with

$$E_{g,n} = \frac{\hbar^2 k_n^2}{2m}, \quad E_{r,n} = \frac{\hbar^2 (\mathbf{k}_n + \mathbf{k}_R)^2}{2m}. \quad (49)$$

In Eq. (27),  $\sum_n p_n$  expresses the thermal average. For high enough temperature  $T$  or for large enough quantization volume  $\mathcal{V}$ , we approximate the parameter  $\mathbf{k}_n$  as continuous with probability density

$$p(\mathbf{k}) = \frac{e^{-k^2/2\sigma_k^2}}{(2\pi\sigma_k^2)^{3/2}}, \quad \sigma_k = \frac{\sqrt{mk_B T}}{\hbar} = \frac{\sqrt{2\pi}}{\lambda_{\text{dB}}}. \quad (50)$$

Equation (27) with  $\sum_n p_n$  approximated as  $\int d^3k p(\mathbf{k})$  yields  $C(t) = e^{-i\hbar k_R^2 t/2m} e^{-t^2/2\tau_R^2}$  so that Eq. (26) yields (see also Refs. [13,22,23])

$$\frac{\eta(t)}{\eta_0} = e^{-t^2/\tau_R^2}, \quad \tau_R = \frac{1}{k_R \sigma_v}, \quad (51)$$

where  $\sigma_v = \hbar\sigma_k/m = \sqrt{k_B T/m}$  is the 1D rms width of the thermal velocity distribution.  $\eta(t)/\eta_0$  displays a Gaussian decay with  $1/e$  time  $\tau_R$ . The expression for  $\tau_R$  can be interpreted as the condition that the typical distance  $\sigma_v \tau_R$  traveled because of thermal motion equals the reduced wavelength  $\lambda_R/2\pi = 1/k_R$  of the spin wave.

##### B. Relation to the spatial coherence function

Alternatively,  $\tau_R$  in Eq. (51) can be written as (see also Ref. [13])

$$\tau_R = \frac{\lambda_{\text{dB}}}{v_R \sqrt{2\pi}}, \quad (52)$$

where  $v_R = \hbar k_R/m$  is the recoil velocity associated with  $\mathbf{k}_R$ . This can be interpreted as the condition that the distance  $v_R \tau_R$  traveled because of the photon recoil equals the coherence length  $l_c = \lambda_{\text{dB}}/\sqrt{2\pi} = 1/\sigma_k$  of the gas. The latter is obtained from the spatial first-order coherence function  $g^{(1)}(r)$ , which has the property [38]

$$|g^{(1)}(r)|^2 = e^{-2\pi r^2/\lambda_{\text{dB}}^2} \quad (53)$$

for a homogeneous, noninteracting gas with  $T$  far above quantum degeneracy.

The appearance of  $g^{(1)}(r)$  in this problem is not a coincidence. In fact, as shown in Ref. [30], the situation considered

here with the purely kinetic dark-time Hamiltonian of Eq. (47) and a plane-wave signal beam  $u(\mathbf{x})$  yields

$$\frac{\eta(t)}{\eta_0} = |g^{(1)}(v_R t)|^2. \quad (54)$$

As discussed in Ref. [30], this holds for an uncorrelated state, such as a noninteracting pure BEC at  $T = 0$  or a thermalized gas with  $T$  far above quantum degeneracy. In addition, it holds for arbitrary separable pure initial states. For other initial states, there might be deviations from this relation, as alluded to in Ref. [30], but a detailed study of such deviations is beyond the present scope. The idea that there is some relation between  $\eta$  and spatial coherence has previously been discussed qualitatively, e.g., in Refs. [21,39]. But we are not aware of a previous derivation of Eq. (54).

For a pure BEC,  $\eta(t)$  decays on a timescale in which  $v_R t$  reaches the sample size, as observed, e.g., in Refs. [21,39]. A much shorter decay time in a gas with a temperature slightly above the critical temperature  $T_C$  for BEC has been observed in Ref. [21]. For nonzero temperatures below  $T_C$ , the coexistence of a BEC and an uncondensed fraction lead to the observation of a bimodal decay [39], qualitatively agreeing with the expectation for the spatial coherence function. However, to our knowledge, quantitative agreement with any model for such a bimodal decay of the retrieval efficiency has not been reported yet.

Equation (45) relates the fringe visibility  $V(t)$  in Ramsey spectroscopy to the efficiency  $\eta(t)$  in EIT-based storage and retrieval. Combination with Eq. (54) suggests that  $V(t)$  should be related to  $|g^{(1)}(v_R t)|$ . Indeed, it is well known that there is some relation between Ramsey spectroscopy and first-order spatial coherence. For example, Ref. [40] used photon recoil in a Ramsey experiment to study the first-order spatial coherence of a BEC, and later Ref. [41] quantitatively derived and experimentally studied the relation between  $g^{(1)}(v_R t)$  and the population transferred after two *resonant* Ramsey pulses. In Ref. [30], we derive the more general relation

$$V(t) = |g^{(1)}(v_R t)| \quad (55)$$

for the fringe visibility  $V$  in Ramsey spectroscopy. This holds for a noninteracting gas as long as the dark-time Hamiltonian is purely kinetic and  $u(\mathbf{x})$  is a plane wave. It applies to arbitrary initial states.

### C. Raman-Nath approximation

We turn to a situation in which atoms in states  $|g\rangle$  and  $|r\rangle$  experience different potentials  $V_g(\mathbf{x})$  and  $V_r(\mathbf{x})$ . The corresponding single-atom dark-time Hamiltonians read

$$H_g = \frac{\mathbf{p}^2}{2m} + V_g(\mathbf{x}), \quad H_r = \frac{\mathbf{p}^2}{2m} + V_r(\mathbf{x}). \quad (56)$$

In our experiment, the potentials  $V_g(\mathbf{x})$  and  $V_r(\mathbf{x})$  are light shifts created if the dipole trap is left on during the dark time, but in general this could also be other potentials, e.g., inhomogeneous Zeeman shifts. Even if both potentials are approximated as harmonic, this is a nontrivial problem, some parts of which have previously been addressed, e.g., in Refs. [15,23–26,42].

In principle, we could calculate  $C(t)$  using Eqs. (27) and (34). However, the resulting calculation will typically become nontrivial because the time evolution of  $|\psi_{r,n}(t)\rangle$  is not given by a trivial phase factor as in Eq. (36). Hence, while Eqs. (27) and (34) can be useful for tackling the problem numerically, that approach will typically not produce a simple analytic result.

Instead, we consider Eq. (29) and apply the Raman-Nath approximation [43] during the dark time. Conceptually, this approximation means that we ignore the distance that an atom travels during the dark time. Technically, this approximation consists in replacing the kinetic-energy operator by a constant real number during the dark time; see, e.g., Ref. [44]. Hence, Eq. (29) becomes

$$C(t) = \sum_n p_n e^{i(E_{\text{kin},g,n} - E_{\text{kin},r,n})t/\hbar} \langle \psi_{g,n}(0) | e^{iV_g t/\hbar} R \times e^{-iV_r t/\hbar} R^\dagger | \psi_{g,n}(0) \rangle, \quad (57)$$

where  $E_{\text{kin},g,n}$  and  $E_{\text{kin},r,n}$  denote the expectation value of the kinetic-energy operator calculated for the states  $|\psi_{g,n}(0)\rangle$  and  $R^\dagger |\psi_{g,n}(0)\rangle$ , respectively. The remaining operators  $V_g$ ,  $V_r$ , and  $R$  are diagonal in the position representation so that

$$C(t) = \sum_n p_n e^{i(E_{\text{kin},g,n} - E_{\text{kin},r,n})t/\hbar} \mathcal{V} \times \int d^3x |v(\mathbf{x}) \psi_{g,n}(\mathbf{x}, 0)|^2 e^{i[V_g(\mathbf{x}) - V_r(\mathbf{x})]t/\hbar}. \quad (58)$$

We assume that for those states  $|\psi_{g,n}(0)\rangle$ , which contribute noticeably to the thermal average, we can approximate  $E_{\text{kin},g,n} = E_{\text{kin},r,n}$  because the typical kinetic energy in state  $|g\rangle$  exceeds other effects, namely the kinetic energy associated with the total photon recoil and with the finite signal-beam waist because of the position-momentum uncertainty relation. Hence

$$C(t) = \mathcal{V} \int d^3x \varrho_g(\mathbf{x}, 0) |v(\mathbf{x})|^2 e^{i[V_g(\mathbf{x}) - V_r(\mathbf{x})]t/\hbar}, \quad (59)$$

with  $\varrho_g(\mathbf{x}, t)$  from Eq. (42). The efficiency  $\eta(t)$  is calculated by inserting  $\mu(t)$  from Eq. (41) and  $C(t)$  from Eq. (59) into Eq. (40). The energy eigenstates of the potential  $V_g(\mathbf{x})$  no longer appear individually in Eqs. (41) and (59). Instead, only  $\varrho_g(\mathbf{x}, t)$  appears, thus often allowing for a simple analytic solution.

To illustrate the plausibility of this result, we consider a Ramsey experiment in which the atoms are subject to a differential potential. For high enough temperature, one can regard the atoms as having classical trajectories. For short enough dark time  $t$  between the two Ramsey pulses, one can assume that the position of each atom is time-independent. In this situation, an atom at position  $\mathbf{x}$  will pick up a differential phase factor  $e^{i[V_g(\mathbf{x}) - V_r(\mathbf{x})]t/\hbar}$ . Averaging over the atomic positions yields a Ramsey pattern with fringe visibility  $V(t) = |\int d^3x \varrho_g(\mathbf{x}) e^{i[V_g(\mathbf{x}) - V_r(\mathbf{x})]t/\hbar}|$ . Obviously, this is closely related to Eq. (59) when keeping Eq. (44) in mind.

### D. Harmonic potential and gravitational sag

We now apply the Raman-Nath approximation to a situation in which both potentials  $V_g(\mathbf{x})$  and  $V_r(\mathbf{x})$  can be approximated as harmonic and in which  $V_g(\mathbf{x})$  is identical before and

after storage and the system is in thermal equilibrium with  $T$  far above quantum degeneracy before storage. As previously discussed in Sec. II C, gravitational sag of the cloud in the trapping potential is a crucial aspect because it causes the position dependence of the differential light shift at cloud center to be linear, which leads to much faster decay of the retrieval efficiency compared to a purely quadratic differential potential.

We assume that both potentials  $V_g(\mathbf{x})$  and  $V_r(\mathbf{x})$  are light-shift potentials created by a traveling Gaussian light beam with wave vector along the  $z$  axis used for dipole trapping the ground state. We obtain light-shift potentials [45]  $V_{j,\text{light}}(\mathbf{x}) = -\alpha_j I(\mathbf{x})/2\epsilon_0 c$ , where  $\alpha_j$  is the dynamical polarizability of state  $j \in \{g, r\}$ ,  $I(\mathbf{x})$  is the trapping-light intensity,  $\epsilon_0$  is the vacuum permittivity, and  $c$  is the vacuum speed of light. A harmonic approximation around the trap center yields  $V_{j,\text{light}}(\mathbf{x}) = V_{j,0} + \kappa_j(x^2 + y^2)/2$ , where  $V_{j,0} = V_{j,\text{light}}(\mathbf{0})$  is the peak value of the trapping potential,  $\kappa_j = -4V_{j,0}/w_r^2$  is the spring constant, and  $w_r$  is the beam waist of the dipole trapping beam. Here, we neglected the divergence of the Gaussian dipole-trapping beam.

Adding the gravitation potential  $mgx$ , we obtain the total potentials  $V_j(\mathbf{x}) = \kappa_j[(x + x_{j,s})^2 + y^2]/2$ , where  $x_{j,s} = mg/\kappa_j$  is the gravitational sag and we used an interaction picture to reset the zero of energy for each internal state individually. We now reset the coordinate origin along the  $x$  axis to obtain

$$V_g(\mathbf{x}) = \frac{\kappa_g}{2}(x^2 + y^2), \quad (60a)$$

$$V_r(\mathbf{x}) = \frac{\kappa_r}{2}[(x - x_0)^2 + y^2], \quad (60b)$$

where  $x_0 = x_{g,s} - x_{r,s}$  is the differential gravitational sag. Note that an atom in state  $|r\rangle$  localized at  $\mathbf{x} = \mathbf{0}$  experiences a force

$$F = \kappa_r x_0 = \frac{\kappa_r - \kappa_g}{\kappa_g} mg \quad (61)$$

along  $x$ .

We assume that before storage the system is in thermal equilibrium at temperature  $T$ . This requires  $\kappa_g \geq 0$ , whereas  $\kappa_r$  may have either sign. We assume that  $T$  is far above quantum degeneracy. Hence, the single-particle atomic density is

$$\varrho_g(\mathbf{x}, 0) = \frac{1}{2\pi\sigma_x^2 L_z} e^{-(x^2+y^2)/2\sigma_x^2} \quad (62)$$

with  $\sigma_x = (\beta\kappa_g)^{-1/2}$ .

We assume that the signal-beam profile is Gaussian,

$$u(\mathbf{x}) = \frac{1}{\sqrt{\mathcal{V}_G}} e^{-(x^2+y^2)/w^2} e^{ik_s z}, \quad (63)$$

where  $w$  is the beam waist and  $\mathcal{V}_G = \pi w^2 L_z/2$  a normalization factor with the dimension of a volume. Here, we consider a cuboidal quantization volume  $\mathcal{V}$  with edge lengths  $L_x$ ,  $L_y$ , and  $L_z$ , and we assumed  $w \ll L_x = L_y$ . In addition, we neglected the divergence of the Gaussian signal beam, the curvature of the wave fronts, and the Gouy phase, all based on the assumption that  $z_R \ll L_z$ , where  $z_R = \kappa_s w^2/2$  is the Rayleigh length.

Using the Raman-Nath approximation (59) in this situation and combining it with Eq. (43) yields

$$\frac{\eta(t)}{\eta_0} = \frac{1}{|\zeta_1|^2} \exp\left(-\frac{t^2}{\tau_F^2} \frac{1}{|\zeta_1|^2}\right), \quad (64)$$

where we abbreviated

$$\tau_F = \frac{2\hbar}{w_r|F|}, \quad w_r = \left(\frac{1}{4\sigma_x^2} + \frac{1}{w^2}\right)^{-1/2} \quad (65)$$

and

$$\zeta_1(t) = 1 - i\frac{t}{\tau_\kappa}, \quad \tau_\kappa = \frac{4\hbar}{w_r^2|\kappa_g - \kappa_r|}. \quad (66)$$

$w_r$  is the radius of the part of the atom cloud that is transferred to the state  $|r\rangle$ . If  $w$  and  $2\sigma_x$  differ by a large factor, then  $w_r$  equals the smaller of these quantities. For later reference, we use  $\kappa_r/\kappa_g = \alpha_r/\alpha_g$  and Eq. (61) to rewrite

$$\tau_\kappa = \frac{4\hbar}{w_r\kappa_g|1 - \frac{\alpha_r}{\alpha_g}|}, \quad \tau_F = \frac{2\hbar}{mgw_r|1 - \frac{\alpha_r}{\alpha_g}|}. \quad (67)$$

Note that taking the finite value of  $w_r$  into account is crucial here, because in the limit  $w_r \rightarrow \infty$ , Eq. (67) yields  $\tau_\kappa \rightarrow 0$  and  $\tau_F \rightarrow 0$ . To make this plausible, note that coherent directed retrieval will be possible if the momentum spread of a pure single-atom state  $|\psi_{r,n}(0)\rangle$  is larger than the differential change in momentum experienced during the dark time in the presence of the potential. Otherwise, the single-atom states  $|\psi_{r,n}(t)\rangle$  and  $R^\dagger|\psi_{g,n}(t)\rangle$  have poor overlap in momentum space, causing  $Q_n(t)$  and  $C(t)$  to vanish according to Eqs. (20) and (27). For a finite  $w_r$ , the position-momentum uncertainty relation enforces a nonzero momentum spread  $2\hbar/w_r$  of each state  $|\psi_{r,n}(0)\rangle$ , thus causing a nonzero time for the decay of  $|C(t)|$ . Note that only the differential potential  $V_r(\mathbf{x}) - V_g(\mathbf{x})$  is relevant for the directed retrieval because only this appears in Eq. (59). In an experiment, the finite value of  $w_r$  has contributions from the initial size  $\sigma_x$  of the ground-state sample and from the transverse beam profiles of the signal and coupling beams. In EIT storage experiments, the signal beam waist typically is the smallest of these length scales because otherwise one cannot achieve high storage efficiency. Note that this is why we approximate the coupling beam as a plane wave throughout this work.

The Raman-Nath approximation is a good approximation as long as the distance that an atom travels during the dark time is small. In a harmonic differential potential, the dark time must be short compared to an oscillation period in the differential potential

$$t \ll 2\pi \sqrt{\frac{m}{|\kappa_r - \kappa_g|}}. \quad (68)$$

In addition, the Raman-Nath approximation neglects the distances traveled because of the initial thermal velocity, the net photon recoil, and the kinetic energy associated with the finite signal-beam waist because of the position-momentum uncertainty relation. This additionally requires  $t \ll w_r/2\sigma_v$ ,  $t \ll w_r/2v_R$ , and  $t \ll mw_r^2/4\hbar$ .

If the gravitational sag is much smaller than the cloud size  $x_{g,s} \ll w_r/2$ , then the gravitational sag has a negligible effect. In this case, the model can be simplified by setting

$F = 0$ . In general, for  $F = 0$  we would expect the differential potential to excite the monopole mode, also known as the breathing mode, of the atomic cloud. If the spring constant should be negative, then the breathing mode would have imaginary frequency corresponding to exponential decay or growth instead of an oscillation. The short-time behavior of this is captured by the Raman-Nath approximation.

For  $F = 0$ , Eq. (64), which relies on the Raman-Nath approximation, yields an algebraic decay

$$\frac{\eta(t)}{\eta_0} = \frac{1}{1 + t^2/\tau_\kappa^2}. \quad (69)$$

A previous analysis of the  $F = 0$  scenario by Kuhr *et al.* [24] used a different approximation, which holds in a parameter regime different from ours and yields a different result, as detailed in Ref. [30].

To make the decay time  $\tau_\kappa$  from Eq. (66) appearing in Eq. (69) plausible, we consider an atom in state  $|r\rangle$  that has a certain momentum and a certain position with  $y = 0$  and arbitrary  $x$  at the beginning of the dark time. According to Eq. (60), it experiences a differential force along the  $x$  axis of

$$-\partial_x(V_r - V_g) = (\kappa_g - \kappa_r)x + F \quad (70)$$

with  $F$  from Eq. (61). After the dark time  $t$ , the differential atomic momentum has changed by  $(\kappa_g - \kappa_r)xt$ , where we used  $F = 0$  and assumed that  $x$  is unchanged because of the Raman-Nath approximation. Equating the modulus of this momentum change with the momentum width  $2\hbar/w_r$  of state  $|\psi_{r,n}(0)\rangle$  and replacing  $x$  by the typical value  $w_r/2$  yields  $t = \tau_\kappa$ .

Conversely, if we assume that the gravitational sag is much larger than the cloud size, then the harmonic part of the differential potential has little effect and we expect the differential potential to excite the dipole mode, also known as the sloshing mode, of the atomic cloud. Again, the short-time behavior of this is captured by the Raman-Nath approximation.

The condition that the gravitational sag is much larger than the cloud size  $w_r/2 \ll x_{g,s}$  is equivalent to  $\tau_F \ll \tau_\kappa$ . This is plausible because if the cloud size  $w_r/2$  is much smaller than the gravitational sag  $x_{g,s}$ , then the atomic cloud in state  $|r\rangle$  essentially experiences a constant force  $F$ , i.e., the term  $\propto x$  in Eq. (70) is negligible. If we consider  $\tau_F \ll \tau_\kappa$ , then the initial decay of  $\eta(t)/\eta_0$  in Eq. (64) from unity to a value much smaller than unity will be well approximated by

$$\frac{\eta(t)}{\eta_0} = \exp\left(-\frac{t^2}{\tau_F^2}\right). \quad (71)$$

This is a good approximation except for the long-time tail of the decay, which is often of little interest because here  $\eta(t)/\eta_0 \ll 1$  anyway.

To make the decay time  $\tau_F$  appearing in Eq. (71) plausible, we consider an atom in state  $|r\rangle$  which has a certain momentum at the beginning of the dark time. After the dark time, its momentum has changed by  $Ft$ . Equating the modulus of this with the momentum width  $2\hbar/w_r$  of state  $|\psi_{r,n}(0)\rangle$  yields  $t = \tau_F$ .

For the parameters of our experiment, the gravitational sag is larger than the size of the cloud so that the linear potential dominates and the atoms hardly sample the curvature

of the differential potential. Hence, Eq. (71) is applicable and the quadratic potential has a negligible effect. Neglecting the quadratic potential from the start drastically simplifies the original problem and makes it possible to solve the problem analytically without resorting to the Raman-Nath approximation. In particular, this allows it to take the two-photon recoil  $\hbar k_R$  and the nonzero initial temperature  $T$  of the atomic cloud into account, which we neglected in the Raman-Nath approximation. This is detailed in Ref. [30].

We note that it might be tempting to associate the in-trap decoherence with a Markovian process driven by random motion of atoms in the trap. However, that ansatz would predict an exponential decay in time, which is in conflict with Eq. (64). The Markovian ansatz is not a good approximation because the atomic motion is not truly randomized on a short enough timescale.

## V. CONCLUSIONS

To conclude, we studied the dark-time decay of the retrieval efficiency for light stored using Rydberg EIT. We experimentally demonstrated a  $1/e$  time of  $30 \mu\text{s}$  in free expansion at low atomic density and low temperature. Our experimental data, both inside the dipole trap and in free expansion, agree well with a model that we presented that showed that it bears analogies to DLCZ single-photon sources and to the decay of fringe visibility in Ramsey spectroscopy. We also experimentally studied the decay of the degree to which the retrieved light is coherent. The model suggests that the trap-induced part of the decay of the retrieval efficiency should become negligible when moving from the present red-detuned 1064 nm dipole trap to a blue-detuned 532 nm dipole trap. This prediction is promising for future experiments aiming for a Rydberg cavity gate.

Another interesting perspective would be to extend the theoretical and experimental studies regarding the spatial coherence function and Ramsey spectroscopy beyond uncorrelated states. Thermalized correlated states might be particularly interesting, i.e., a noninteracting ensemble of identical fermions at zero temperature or a noninteracting thermalized gas of bosons or fermions at a nonzero temperature, which is not far above quantum degeneracy.

## ACKNOWLEDGMENTS

We thank Johannes Otterbach, Thomas Pohl, and Richard Schmidt for discussions. This work was supported by Deutsche Forschungsgemeinschaft under Germany's excellence strategy via Nanosystems Initiative Munich and Munich Center for Quantum Science and Technology and under priority program 1929 GiRyd. T.S. acknowledges support from Studienstiftung des Deutschen Volkes.

## APPENDIX A: ATOM-LIGHT INTERACTION HAMILTONIAN

In this Appendix, we present details regarding the atom-light interaction Hamiltonian  $\mathcal{V}_{\text{al}}$  appearing in Eq. (12). We assume that a signal (coupling) light field with angular frequency  $\omega_s > 0$  ( $\omega_c > 0$ ) and single-photon detuning  $\Delta_s =$

$\omega_s - \omega_{eg}$  ( $\Delta_c = \omega_c - \omega_{re}$ ) is near resonant with the  $|g\rangle \leftrightarrow |e\rangle$  ( $|e\rangle \leftrightarrow |r\rangle$ ) transition with dipole matrix element  $d_{eg}$  ( $d_{re}$ ) and atomic resonance angular frequency  $\omega_{eg}$  ( $\omega_{re}$ ). We describe the coupling light field as a classical plane wave with  $E_c(\mathbf{x}, t) = \frac{1}{2}E_{c,0}e^{-i\omega_c t + i\mathbf{k}_c \cdot \mathbf{x}} + \text{c.c.}$  with wave vector  $\mathbf{k}_c$ , complex amplitude  $E_{c,0}$ , and Rabi frequency  $\Omega_c = -d_{re}E_{c,0}/\hbar$ .

The signal light field, however, must be quantized to obtain a useful description of EIT-based storage because it is crucial that an atomic excitation from state  $|g\rangle$  to  $|e\rangle$  has a backaction onto the signal light field, reducing its photon number by 1. We include only a single monochromatic optical mode of the signal field in our model. The operator describing its electric field is  $\hat{E}(\mathbf{x}) = \hat{E}^{(+)}(\mathbf{x}) + \text{H.c.}$ , where  $\hat{E}^{(+)}(\mathbf{x}) = E_{\omega_s} \sqrt{\mathcal{V}} u(\mathbf{x}) \hat{a}_s$  would become the positive-frequency component if one used the Heisenberg picture,  $E_{\omega_s} = \sqrt{\hbar\omega_s/2\epsilon_0\mathcal{V}}$  is the field amplitude,  $\mathcal{V}$  is the quantization volume,  $u(\mathbf{x})$  is the spatial mode function normalized to  $\int_{\mathcal{V}} d^3x |u(\mathbf{x})|^2 = 1$ , and  $\hat{a}_s$  is the annihilation operator for a photon in this mode with bosonic commutation relation  $[\hat{a}_s, \hat{a}_s^\dagger] = 1$ . Using  $E_{\omega_s}$  one introduces  $g_R = -d_{eg}E_{\omega_s}/\hbar$ , which is half the vacuum Rabi frequency.

We use an interaction picture and the rotating-wave approximation. We find that the Hamiltonian for the  $i$ th atom contains a modified internal-energy term  $H_{\text{int},i} = \hbar\Delta_s |g_i\rangle\langle g_i| - \hbar\Delta_c |r_i\rangle\langle r_i|$  together with the potential  $V_{\text{al},i}$  describing the atom-light interaction with position representation,

$$V_{\text{al},i}(\mathbf{x}_i) = \hbar g_R \sqrt{\mathcal{V}} u(\mathbf{x}_i) \hat{a}_s |e_i\rangle\langle g_i| + \frac{\hbar}{2} \Omega_c e^{i\mathbf{k}_c \cdot \mathbf{x}_i} |r_i\rangle\langle e_i| + \text{H.c.} \quad (\text{A1})$$

The total atom-light interaction Hamiltonian is  $\mathcal{V}_{\text{al}} = \sum_{i=1}^N V_{\text{al},i}$ . Spontaneous emission from state  $|e\rangle$  into modes orthogonal to  $u(\mathbf{x})$  is not included in  $\mathcal{V}_{\text{al}}$ . In the following, we always assume that  $g_R$  and  $\Omega_c$  are real and that  $\Delta_s = \Delta_c = 0$ . Reference [3] uses the notation  $\Omega$ , where we use  $\Omega_c/2$ .

Had we considered a  $\Lambda$ -type level scheme instead of the ladder-type level scheme, i.e., if state  $|r\rangle$  had an energy lower than the energy of state  $|e\rangle$ , then we would have to replace  $\Omega_c \mapsto \Omega_c^*$  and along with it  $\mathbf{k}_c \mapsto -\mathbf{k}_c$  and  $\Delta_c \mapsto -\Delta_c$ . Everything else would remain unchanged.

Note that, strictly speaking, the positive-frequency component of the quantized electric field is  $\hat{E}^{(+)}(\mathbf{x}) = \sum_m E_{\omega_m} \sqrt{\mathcal{V}} u_m(\mathbf{x}) \hat{a}_m$ , where the  $u_m(\mathbf{x})$  form an orthonormal basis of mode functions. Each  $u_m(\mathbf{x})$  must be a monochromatic solution to the wave equation in classical electrodynamics. The corresponding angular frequency is  $\omega_m$ , and this yields  $E_{\omega_m} = \sqrt{\hbar\omega_m/2\epsilon_0\mathcal{V}}$ . Additionally, each  $u_m(\mathbf{x})$  must meet some boundary condition imposed by the quantization volume. Apart from that, one can choose the  $u_m(\mathbf{x})$  in an arbitrary fashion. The  $\hat{a}_m$  are the corresponding bosonic photon annihilation operators.

As in Ref. [3], we keep only one term in this sum, namely the one with  $u(\mathbf{x})$ . The special treatment of this mode is justified because upon retrieval this term gives rise to directed emission because of constructive interference. The collection of all other modes gives rise to undirected retrieval. As we are not interested in the fate of those photons emitted in an undirected fashion, we can trace over them. This leaves us with a corresponding term in the dissipator of a quantum

master equation, describing the atomic decay with rate coefficient  $\Gamma_e$  which accompanies the spontaneous emission into those modes.

As a further approximation, we use the resulting Hamiltonian with just one term even when  $u(\mathbf{x})$  is a Gaussian beam that solves the wave equation only in paraxial approximation and also meets the boundary condition only in an approximate fashion. This is justified as long as the waist is much larger than the wavelength of the signal light because otherwise the paraxial approximation becomes poor.

## APPENDIX B: RETRIEVAL EFFICIENCY

In this Appendix, we derive the central result (19) for the retrieval efficiency for a separable pure initial state. For brevity, we drop the thermal averaging index  $n$  from the notation throughout this Appendix. We start by constructing an explicit expression for the projector  $\mathcal{P}_u$ . To this end, we consider an orthonormal basis of external states of the  $i$ th atom ( $|\phi_{1,i}\rangle, |\phi_{2,i}\rangle, |\phi_{3,i}\rangle, \dots$ ). Hence, the product states  $\bigotimes_{i=1}^N |\phi_{j_i,i}\rangle$  form an orthonormal basis of the Hilbert space  $\mathcal{H}_{\text{ext}}$  of all external  $N$ -atom states. Similarly, the product states

$$|\Phi_{g,j_1,j_2,\dots,j_N}, 1_s\rangle = |1_s\rangle \bigotimes_{i=1}^N |\phi_{j_i,i}, g_i\rangle \quad (\text{B1})$$

form an orthonormal basis of the subspace of states with one signal photon and zero atomic excitations. Likewise, the states  $|\phi_{j_i,i}, r_i\rangle \bigotimes_{i'=1, i' \neq i}^N |\phi_{j_{i'},i'}, g_{i'}\rangle$  form an orthonormal basis of the subspace of states with one Rydberg excitation. Note that there are  $N$  options for which of the atoms is excited. Since  $R_i$  is unitary, we can alternatively use the states

$$(R_i^\dagger |\phi_{j_i,i}, r_i\rangle) \bigotimes_{\substack{i'=1 \\ i' \neq i}}^N |\phi_{j_{i'},i'}, g_{i'}\rangle \quad (\text{B2})$$

as an orthonormal basis of the subspace of states with one Rydberg excitation. Again, there are  $N$  options for which of the atoms is excited.

For a given  $u(\mathbf{x})$ , each of the states  $|\Phi_{g,j_1,j_2,\dots,j_N}, 1_s\rangle$  has a 3D invariant subspace with a single excitation associated with it in analogy to Sec. III A. Within each of these 3D subspaces, there is a symmetric Dicke state with one Rydberg excitation,

$$|\Phi_{r,j_1,j_2,\dots,j_N}\rangle = \frac{1}{\sqrt{N}} \sum_{i=1}^N (R_i^\dagger |\phi_{j_i,i}, r_i\rangle) \bigotimes_{\substack{i'=1 \\ i' \neq i}}^N |\phi_{j_{i'},i'}, g_{i'}\rangle. \quad (\text{B3})$$

The states  $|\Phi_{r,j_1,j_2,\dots,j_N}\rangle$  form an orthonormal basis of the subspace  $W_u$ . Hence

$$\mathcal{P}_u = \sum_{j_1,j_2,\dots,j_N} |\Phi_{r,j_1,j_2,\dots,j_N}\rangle \langle \Phi_{r,j_1,j_2,\dots,j_N}|. \quad (\text{B4})$$

Note that the dimension of the subspace  $W_u$  is a factor of  $N$  smaller than the dimension of the subspace spanned by the states in Eq. (B2) because among the  $N$  options for which of the atoms is excited, only one superposition is realized, namely the symmetric Dicke state that couples to mode  $u(\mathbf{x})$ .

To determine the retrieval efficiency based on Eq. (18), we first need to calculate  $\mathcal{P}_u |\Psi_r(t)\rangle$ . We facilitate this calculation



by choosing the orthonormal basis ( $|\phi_{1,i}\rangle, |\phi_{2,i}\rangle, |\phi_{3,i}\rangle, \dots$ ) in a way that is adapted to the problem. Specifically, we construct this basis such that

$$|\phi_{1,i}\rangle = |\psi_{g,i}(t)\rangle \quad (\text{B5})$$

and that  $R_i|\psi_{r,i}(t)\rangle$  lies in the two-dimensional (2D) subspace spanned by  $|\phi_{1,i}\rangle$  and  $|\phi_{2,i}\rangle$ . We denote the corresponding expansion coefficients as  $Q_i(t)$  and  $G_i(t)$ , defined by

$$R_i|\psi_{r,i}(t)\rangle = Q_i(t)|\phi_{1,i}\rangle + G_i(t)|\phi_{2,i}\rangle. \quad (\text{B6})$$

Note that this agrees with the definition of  $Q_i(t)$  in Eq. (20). In addition, as  $R_i$  is unitary and  $|\psi_{r,i}(t)\rangle$  is properly normalized,

$$|Q_i|^2 + |G_i|^2 = 1. \quad (\text{B7})$$

Combining Eqs. (17), (B3), (B5), and (B6) yields

$$\begin{aligned} & \langle \Phi_{r,j_1,j_2,\dots,j_N} | \Psi_r(t) \rangle \\ &= \frac{1}{N} \sum_{i=1}^N \underbrace{\langle \phi_{j_i,i} | R_i | \psi_{r,i}(t) \rangle}_{=Q_i\delta_{1,j_i}+G_i\delta_{2,j_i}} \prod_{\substack{i'=1 \\ i' \neq i}}^N \underbrace{\langle \phi_{j_{i'},i'} | \psi_{g,i'}(t) \rangle}_{=\delta_{1,j_{i'}}}. \end{aligned} \quad (\text{B8})$$

Insertion into Eq. (B4) yields

$$\begin{aligned} \mathcal{P}_u |\Psi_r(t)\rangle &= |\Phi_{r,1,\dots,1}\rangle \frac{1}{N} \sum_{i=1}^N Q_i \\ &+ \sum_{i=1}^N |\Phi_{r,1,\dots,1,j_i=2,1,\dots,1}\rangle \frac{1}{N} G_i. \end{aligned} \quad (\text{B9})$$

Combining with Eq. (18) yields

$$\frac{\eta(t)}{\eta_0} = \frac{1}{N^2} \left| \sum_{i=1}^N Q_i \right|^2 + \frac{1}{N^2} \sum_{i=1}^N |G_i|^2. \quad (\text{B10})$$

For  $N \gg 1$  this yields Eq. (19) because  $\frac{1}{N^2} \sum_{i=1}^N |G_i|^2 \leq \frac{1}{N} \max_i |G_i|^2 = O(\frac{1}{N})$ . As a result, the only term in  $\mathcal{P}_u |\Psi_r(t)\rangle$  that gives a non-negligible contribution to  $\eta(t)$  for  $N \gg 1$  comes from  $|\Phi_{r,1,\dots,1}\rangle$ , which equals  $|\Phi(t)\rangle$  from Eq. (22). Hence for  $N \gg 1$ ,

$$\mathcal{P}_u |\Psi_r(t)\rangle = |\Phi(t)\rangle \langle \Phi(t) | \Psi_r(t) \rangle. \quad (\text{B11})$$

Inserting this into Eq. (18) yields Eq. (21).

In principle, the state in Eq. (B9) is entangled and it would remain entangled during the adiabatic passage from  $\vartheta = \pi/2$  to 0, but for  $N \gg 1$  we obtain Eq. (B11), which becomes a product state  $|\Phi_{g,1,\dots,1}, 1_s\rangle$  during the adiabatic passage from  $\vartheta = \pi/2$  to 0. Hence, as a byproduct of our calculation, we obtained the final  $N$ -atom state after retrieval, at least for those cases in which retrieval occurs into mode  $u(\mathbf{x})$ .

In our experiment, we use an optical fiber for transverse mode selection of the retrieved light. However, we do not select the longitudinal mode. Within our model, this lack of longitudinal mode selection has no effect on the efficiency. To see this, we use the fact that  $u(\mathbf{x})$  has a plane-wave-type dependence on  $z$ , and we assume that  $V_g(\mathbf{x})$  and  $V_r(\mathbf{x})$  are independent of  $z$ . Hence, starting from thermal equilibrium, the initial atomic wave function  $\psi_{g,n,i}(\mathbf{x}, 0)$  has a plane-wave-type dependence on  $z$ . Hence, the longitudinal mode along  $z$  is unchanged when calculating  $U_{g,i}^\dagger(t) R_i U_{r,i}(t) R_i^\dagger |\psi_{g,i}(0)\rangle$ , which is

relevant for Eq. (20). In essence, this reflects conservation of linear momentum along  $z$  because the momentum added during the transition  $|g\rangle \rightarrow |r\rangle$  is removed in the transition  $|r\rangle \rightarrow |g\rangle$ .

The following consideration will show why a state orthogonal to  $W_u$  does not couple to the mode  $u(\mathbf{x})$ . We start by considering the state  $|\Psi_{g,\text{in}}, 1_s\rangle$  of Eq. (8a). Taking photon recoil for a given  $u(\mathbf{x})$  into account, it is obvious that a transition of the  $i$ th atom from internal state  $|g_i\rangle$  to  $|r_i\rangle$  must change its external state from  $|\psi_{g,i}(0)\rangle$  to  $|\psi_{r,i}(0)\rangle$ . When considering  $N$  atoms, there is a corresponding  $N$ -dimensional subspace with one Rydberg excitation. It is spanned by the orthonormal basis  $|\psi_{r,i}(0), r_i\rangle \otimes_{i'=1, i' \neq i}^N |\psi_{g,i'}(0), g_{i'}\rangle$  with  $i \in \{1, 2, \dots, N\}$ . However,  $\mathcal{V}_{\text{al}}$  couples the mode  $u(\mathbf{x})$  only to the symmetric Dicke state of Eq. (8c). The  $(N-1)$ -dimensional subspace orthogonal thereto does not couple to the mode  $u(\mathbf{x})$ . For an arbitrary initial state, this statement generalizes to the fact that a state orthogonal to  $W_u$  does not couple to the mode  $u(\mathbf{x})$ .

The state after storage,  $|\Psi_r(0)\rangle$ , is an element of  $W_u$ . The dark-time evolution rotates this state inside the subspace spanned by the states in Eq. (B2). Whenever  $\eta(t) < \eta_0$ , this rotated state  $|\Psi_r(t)\rangle$  has a nonzero component orthogonal to  $W_u$ . When the coupling light is turned back on for retrieval, this component causes spontaneous emission into modes orthogonal to  $u(\mathbf{x})$ . The fate of those excitations is beyond the scope of the present paper. They are simply regarded as lost.

### APPENDIX C: ENTANGLED INITIAL STATES

This Appendix discusses a straightforward generalization of the model to arbitrary initial states. Again, the initial density matrix can be expanded as in Eq. (6) but now each pure state  $|\Psi_{g,n,\text{in}}\rangle$  can be entangled, i.e., nonseparable. This expansion is possible because  $\rho_{N,\text{in}}$  is Hermitian so that it can be diagonalized.

Hence, Eq. (7) still holds but we need to generalize the calculation of  $\eta_n(t)$  to entangled pure states. To this end, we expand the entangled pure state  $|\Psi_{g,n,\text{in}}\rangle$  in an orthonormal set of separable pure states  $|\Psi_{g,n,m,\text{in}}\rangle$  as

$$|\Psi_{g,n,\text{in}}\rangle = \sum_m c_{n,m} |\Psi_{g,n,m,\text{in}}\rangle \quad (\text{C1})$$

with

$$\langle \Psi_{g,n,m,\text{in}} | \Psi_{g,n,m',\text{in}} \rangle = \delta_{m,m'}. \quad (\text{C2})$$

Hence, the complex expansion coefficients  $c_{n,m}$  fulfill  $\sum_m |c_{n,m}|^2 = 1$ . This expansion is possible because any Hilbert space has an orthonormal basis of separable pure states.

The treatment of storage and retrieval for each separable pure initial state  $|\Psi_{g,n,m,\text{in}}\rangle$  is identical to the above. In particular, Eq. (B11), which holds for  $N \gg 1$ , now simply picks up an additional index  $m$ , thus becoming

$$\mathcal{P}_u |\Psi_{r,n,m}(t)\rangle = |\Phi_{n,m}(t)\rangle \langle \Phi_{n,m}(t) | \Psi_{r,n,m}(t) \rangle, \quad (\text{C3})$$

where  $|\Psi_{r,n,m}(t)\rangle$  and  $|\Phi_{n,m}(t)\rangle$  are defined in analogy to the above, starting from the separable pure state  $|\Psi_{g,n,m,\text{in}}\rangle$ . For clarity, Eq. (C3) explicitly includes the index  $n$ , which was omitted in Appendix B for brevity. Note that  $R_i$  is unitary

and that the dark-time evolution is unitary. Hence, Eq. (C2) implies

$$\langle \Phi_{n,m}(t) | \Phi_{n,m'}(t) \rangle = \delta_{m,m'}. \quad (\text{C4})$$

The discussion leading to Eq. (18) relies on adiabatic following but it is irrelevant whether the initial pure state is entangled. Hence, Eq. (18) is applicable here for calculating  $\eta_n(t)$  for the possibly entangled pure state  $|\Psi_{g,n,\text{in}}\rangle$ . In addition, it is applicable for calculating  $\eta_{n,m}(t)$  for the separable pure state  $|\Psi_{g,n,m,\text{in}}\rangle$ . Combining this with Eqs. (C1), (C3), and (C4) and with the fact that  $\mathcal{P}_u$  is linear yields

$$\eta_n(t) = \sum_m |c_{n,m}|^2 \eta_{n,m}(t). \quad (\text{C5})$$

This is the weighted average of the efficiencies  $\eta_{n,m}(t)$ .

For the special case of a thermalized initial state of noninteracting atoms, each  $|\Psi_{g,n,\text{in}}\rangle$  is a bosonically symmetrized or fermionically antisymmetrized version of one separable pure state. Hence, all the values of  $\eta_{n,m}(t)$  for a given  $n$  are independent of  $m$ , and the averaging in Eq. (C5) becomes trivial.

There is a caveat here. If one considers a degenerate Fermi gas, which is an example of an entangled state, then Eq. (18) might become a poor approximation for the retrieval efficiency. This is because if just before retrieval an external single-atom state is already occupied by a ground-state atom, then Pauli blocking will prohibit the transition of another atom to this final state. This might result in a suppression of the directed retrieval.

#### APPENDIX D: BEYOND PLANE WAVES

In this Appendix, we present details regarding the generalization beyond a plane-wave signal light field, which was only briefly summarized in Sec. III E. The main difference will be the appearance of several nontrivial normalization factors. Apart from that, the treatment is largely analogous. The main reason for discussing this aspect in an Appendix is that the main text becomes more transparent because the relevant physics is not obscured by a lengthy discussion of all the normalization factors.

We assume that the mode function is of the form  $u(\mathbf{x}) = u_{\perp}(x, y)e^{ik_z z}/\sqrt{L_z}$ , in which the longitudinal mode function remains that of a plane wave but there might be some nontrivial transverse mode function  $u_{\perp}(x, y)$ , such as the Gaussian of Eq. (63). Hence, the longitudinal properties of the signal light remain trivial.

We still define the single-particle states  $|\psi_{e,n,i}(0)\rangle$  and  $|\psi_{r,n,i}(0)\rangle$  by Eq. (9). Hence, Eq. (11) still holds. But now these single-particle states are no longer properly normalized. Instead, calculating their norm squared yields the dimensionless real number

$$\begin{aligned} M_{n,i}(0) &= \langle \psi_{e,n,i}(0) | \psi_{e,n,i}(0) \rangle = \langle \psi_{r,n,i}(0) | \psi_{r,n,i}(0) \rangle \\ &= \mathcal{V} \int_{\mathcal{V}} d^3x |u(\mathbf{x})\psi_{g,n,i}(\mathbf{x}, 0)|^2, \end{aligned} \quad (\text{D1})$$

which describes how well the mode  $u(\mathbf{x})$  overlaps with the atom wave function before storage  $\psi_{g,n,i}(\mathbf{x}, 0)$ .

Using these states, we can easily generalize two of the  $N$ -atom states of Eq. (8) to

$$|\Psi_{e,n}(0)\rangle = \frac{1}{\sqrt{N_n(0)}} \sum_{i=1}^N |\psi_{e,n,i}(0), e_i\rangle \bigotimes_{\substack{i'=1 \\ i' \neq i}}^N |\psi_{g,n,i'}(0), g_{i'}\rangle \quad (\text{D2a})$$

and

$$|\Psi_{r,n}(0)\rangle = \frac{1}{\sqrt{N_n(0)}} \sum_{i=1}^N |\psi_{r,n,i}(0), r_i\rangle \bigotimes_{\substack{i'=1 \\ i' \neq i}}^N |\psi_{g,n,i'}(0), g_{i'}\rangle. \quad (\text{D2b})$$

The only difference from Eq. (8) is the appearance of the dimensionless normalization factor  $N_n(0)$  instead of the atom number  $N$ . The definition of  $|\Psi_{g,n,\text{in}}, 1_s\rangle$  remains unchanged. The  $N$ -atom states  $|\Psi_{e,n}(0)\rangle$  and  $|\Psi_{r,n}(0)\rangle$  in Eq. (D2) are properly normalized because we choose

$$N_n(0) = \sum_{i=1}^N M_{n,i}(0), \quad (\text{D3})$$

which can be regarded as the effective number of atoms coupled to the EIT signal light.

Compared to a plane wave  $u(\mathbf{x})$ , the situation here is conceptually a little more subtle because the 3D subspace spanned by states  $[|\Psi_{g,n,\text{in}}, 1_s\rangle, |\Psi_{e,n}(0)\rangle, |\Psi_{r,n}(0)\rangle]$  is no longer invariant under application of the atom-light interaction potential  $\mathcal{V}_{\text{al}}$ . This is because a transition  $|g\rangle \rightarrow |e\rangle$  is accompanied by multiplication with  $u(\mathbf{x})\sqrt{\mathcal{V}}$  whereas the reverse transition  $|e\rangle \rightarrow |g\rangle$  is accompanied by multiplication with  $u^*(\mathbf{x})\sqrt{\mathcal{V}}$ . If and only if  $u(\mathbf{x})$  is a plane wave, then these factors cancel, which makes the 3D subspace invariant. As argued in Appendix E, we can safely ignore this subtlety and restrict our considerations to only this 3D subspace.

The state after storage is again  $|\Psi_{r,n}(0)\rangle$ . The dark-time evolution proceeds as in the plane-wave case. In particular, Eq. (16) still holds and Eq. (17) becomes

$$\begin{aligned} |\Psi_{r,n}(t)\rangle &= \mathcal{U}_d(t) |\Psi_{r,n}(0)\rangle \\ &= \frac{1}{\sqrt{N_n(0)}} \sum_{i=1}^N |\psi_{r,n,i}(t), r_i\rangle \bigotimes_{\substack{i'=1 \\ i' \neq i}}^N |\psi_{g,n,i'}(t), g_{i'}\rangle. \end{aligned} \quad (\text{D4})$$

Again, this differs from the plane-wave case only in the normalization factor  $N_n(0)$ . Note that the unitary time evolution during the dark time implies that the norm of each  $|\psi_{r,n,i}(t)\rangle$  is time-independent, which is why the normalization factor  $N_n(0)$  appearing in  $|\Psi_{r,n}(t)\rangle$  is also time-independent.

The retrieval is also treated as in the plane-wave case. In particular, Eqs. (18) and (21) remain unchanged and the Dicke state of Eq. (22) is generalized to

$$|\Phi_n(t)\rangle = \frac{1}{\sqrt{N_n(t)}} \sum_{i=1}^N (R_i^\dagger |\psi_{g,n,i}(t), r_i\rangle) \bigotimes_{\substack{i'=1 \\ i' \neq i}}^N |\psi_{g,n,i'}(t), g_{i'}\rangle. \quad (\text{D5})$$

Again, the only difference from the plane-wave case is that the single-atom state  $R_i^\dagger |\psi_{g,n,i}(t)\rangle$  is not normalized, which yields the normalization factor for the  $N$ -atom state

$$N_n(t) = \sum_{i=1}^N M_{n,i}(t) \quad (\text{D6})$$

with the dimensionless real number

$$\begin{aligned} M_{n,i}(t) &= \langle \psi_{g,n,i}(t) | R_i R_i^\dagger | \psi_{g,n,i}(t) \rangle \\ &= \mathcal{V} \int_{\mathcal{V}} d^3x |u(\mathbf{x}) \psi_{g,n,i}(\mathbf{x}, t)|^2. \end{aligned} \quad (\text{D7})$$

In the limit  $t \rightarrow 0$ , the last three equations coincide with Eqs. (D2b), (D3), and (D1). Hence Eq. (21) yields  $\eta_n(0)/\eta_0 = 1$ . In addition, note that  $0 \leq M_{n,i}(t) \leq 1$ . For the special case in which  $u(\mathbf{x})$  or  $\psi_{g,n,i}(\mathbf{x}, t)$  is a plane wave, we obtain  $M_{n,i}(t) = 1$ , and if this applies to all  $i$ , then  $N_n(t) = N$ .

We also find that Eq. (19) is generalized to

$$\frac{\eta_n(t)}{\eta_0} = \frac{1}{N_n(0)N_n(t)} \left| \sum_{i=1}^N Q_{n,i}(t) \right|^2 \quad (\text{D8})$$

and Eq. (20) remains unchanged. In particular, for  $t = 0$  we combine Eqs. (11), (20), and (D1) to obtain

$$Q_{n,i}(0) = M_{n,i}(0), \quad (\text{D9})$$

which again yields  $\eta_n(0)/\eta_0 = 1$ .

For a pure BEC, Eq. (D8) simplifies to

$$\frac{\eta_{\text{BEC}}(t)}{\eta_0} = \frac{|Q(t)|^2}{M(0)M(t)}. \quad (\text{D10})$$

We turn to the uncorrelated state of Eq. (24). Wanting to average  $\eta_n(t)$  over  $n$ , we are facing the difficulty that in  $N_n(t) = \sum_{i=1}^N M_{n,i}(t)$  the sum over  $i$  appears in the denominator in Eq. (D8). To solve this problem, we note that  $N_n(t) = \sum_{i=1}^N M_{n,i}(t)$  for  $N \gg 1$  is the sum over a large number  $N$  of uncorrelated random variables  $M_{n,i}(t)$ , which each have the same mean value

$$\mu(t) = \sum_n p_{n,i} M_{n,i}(t) = \sum_n p_{n,1} M_{n,1}(t) \quad (\text{D11})$$

and the same standard deviation because the particles are identical. The central limit theorem states that  $\frac{1}{N}N_n(t)$  is a normally distributed, random variable with mean value  $\mu(t)$  and a standard deviation of order  $O(N^{-1/2})$ . We consider  $N \gg 1$  and neglect this standard deviation, i.e., we replace  $N_n(t)$  by  $N\mu(t)$  and  $N_n(0)$  by  $N\mu(0)$ . Hence, Eq. (26) generalizes to

$$\frac{\eta(t)}{\eta_0} = \frac{|C(t)|^2}{\mu(0)\mu(t)}, \quad (\text{D12})$$

where Eq. (27) remains unchanged. The quantities  $C(t)$  and  $\mu(t)$  are obtained from  $Q_n(t)$  and  $M_n(t)$  by averaging over  $n$ . As mentioned below Eq. (25), a pure BEC is an example of an uncorrelated state. Hence, Eq. (D12) reproduces Eq. (D10) if the initial state is a pure BEC. Note that Eq. (D9) yields

$$C(0) = \mu(0). \quad (\text{D13})$$

If Eq. (32) holds, i.e., typically because the Hamiltonian is identical before and after storage, then  $M_{n,i}(t) = M_{n,i}(0)$  so that  $\mu(t) = \mu(0)$  and

$$\frac{\eta(t)}{\eta_0} = \left| \frac{C(t)}{C(0)} \right|^2 \quad (\text{D14})$$

and Eqs. (27), (34), and (37) remain unchanged, now with  $\langle \psi_{r,n,i}(0) | \psi_{r,n,i}(0) \rangle = M_n(0)$  according to Eq. (38).

## APPENDIX E: NON-INVARIANCE OF THE SUBSPACE

As mentioned in Appendix D, if  $u(\mathbf{x})$  is not a plane wave, then the 3D subspace spanned by the states  $[|\Psi_{g,n,\text{in}}, 1_s\rangle, |\Psi_{e,n}(0)\rangle, |\Psi_{r,n}(0)\rangle]$  is no longer invariant under application of the atom-light interaction potential  $\mathcal{V}_{\text{al}}$ . In this Appendix, we argue why this is not a major concern.

As an example, we consider application of  $\mathcal{V}_{\text{al}}$  to any vector in this 3D subspace. This will create a vector in a 4D subspace spanned, e.g., by the above three vectors combined with

$$\begin{aligned} |\Psi_{g,n}^{(1)}, 1_s\rangle &= \frac{1}{\sqrt{N_{g,n,i}^{(1)}(0)}} |1_s\rangle \sum_{i=1}^N R_i R_i^\dagger |\psi_{g,n,i}(0), g_i\rangle \\ &\quad \bigotimes_{\substack{i'=1 \\ i' \neq i}}^N |\psi_{g,n,i'}(0), g_{i'}\rangle \end{aligned} \quad (\text{E1})$$

with some normalization factor  $N_{g,n,i}^{(1)}(0)$ . Applying  $\mathcal{V}_{\text{al}}$  to any vector in this 4D subspace yields a vector in a 5D subspace, etc. In this way, we obtain an infinite hierarchy of subspaces.

If we consider the 4D subspace rather than the 3D subspace, then we obtain a negligible correction to the final result  $\eta_n(t)$  of our calculation because the single-atom state of only one atom in  $|\Psi_{g,n}^{(1)}, 1_s\rangle$  differs from  $|\Psi_{g,n,\text{in}}, 1_s\rangle$ . All other single-atom states are identical. Assuming that the number of coupled atoms is large  $N_n(0) \gg 1$ , this difference has a negligible effect. The same applies if we extend the model to the 5D subspace and so forth, unless the number  $k$  of applications of  $V_{eg} = \sum_{i=1}^N \hbar g_R \sqrt{\mathcal{V}} u(\mathbf{x}_i) \hat{a}_s |e_i\rangle \langle g_i| + \text{H.c.}$  becomes comparable to  $N_n(0)$ .

Now, the number  $k$  of applications of  $V_{eg}$  that we need to consider is set by the duration  $t_s$  of the storage pulse. The typical value of  $k$  that needs to be taken into account is twice the number of  $|g\rangle \leftrightarrow |e\rangle$  Rabi flops that the Bloch vector can undergo during time  $t_s$ . Let  $\varphi_R = \sqrt{N_n(0)} g_R t_s$  denote the pulse area. Then the number of Rabi flops is  $\varphi_R/2\pi$ . All states obtained by a much larger number of applications of  $V_{eg}$  have negligible amplitude in the state after storage. To achieve adiabatic following in the dark state during the storage process, we need  $1 \ll \varphi_R/\pi$ . But typically  $N_n(0)$  is large enough that this leaves enough room to choose  $t_s$  such that  $1 \ll \varphi_R/\pi \ll N_n(0)$ . We assume that such a choice was made. Hence, it suffices to restrict  $k$  to  $k \approx \varphi_R/\pi \ll N_n(0)$ . A similar argument applies to the adiabatic passage during retrieval.

- [1] A. I. Lvovsky, B. C. Sanders, and W. Tittel, Optical quantum memory, *Nat. Photon.* **3**, 706 (2009).
- [2] M. Fleischhauer and M. D. Lukin, Dark-State Polaritons in Electromagnetically Induced Transparency, *Phys. Rev. Lett.* **84**, 5094 (2000).
- [3] M. Fleischhauer and M. D. Lukin, Quantum memory for photons: Dark-state polaritons, *Phys. Rev. A* **65**, 022314 (2002).
- [4] C. Liu, Z. Dutton, C. H. Behroozi, and L. V. Hau, Observation of coherent optical information storage in an atomic medium using halted light pulses, *Nature (London)* **409**, 490 (2001).
- [5] D. F. Phillips, A. Fleischhauer, A. Mair, R. L. Walsworth, and M. D. Lukin, Storage of Light in Atomic Vapor, *Phys. Rev. Lett.* **86**, 783 (2001).
- [6] M. Fleischhauer, A. Imamoglu, and J. P. Marangos, Electromagnetically induced transparency: Optics in coherent media, *Rev. Mod. Phys.* **77**, 633 (2005).
- [7] Y. O. Dudin, L. Li, and A. Kuzmich, Light storage on the time scale of a minute, *Phys. Rev. A* **87**, 031801 (2013).
- [8] I. Friedler, D. Petrosyan, M. Fleischhauer, and G. Kurizki, Long-range interactions and entanglement of slow single-photon pulses, *Phys. Rev. A* **72**, 043803 (2005).
- [9] J. D. Pritchard, D. Maxwell, A. Gauguier, K. J. Weatherill, M. P. A. Jones, and C. S. Adams, Cooperative Atom-Light Interaction in a Blocked Rydberg Ensemble, *Phys. Rev. Lett.* **105**, 193603 (2010).
- [10] O. Firstenberg, C. S. Adams, and S. Hofferberth, Nonlinear quantum optics mediated by Rydberg interactions, *J. Phys. B* **49**, 152003 (2016).
- [11] J. B. Balewski, A. T. Krupp, A. Gaj, D. Peter, H. P. Büchler, R. Löw, S. Hofferberth, and T. Pfau, Coupling a single electron to a Bose-Einstein condensate, *Nature (London)* **502**, 664 (2013).
- [12] S. Baur, D. Tiarks, G. Rempe, and S. Dürr, Single-Photon Switch Based on Rydberg Blockade, *Phys. Rev. Lett.* **112**, 073901 (2014).
- [13] S. E. Baur, A single-photon switch and transistor based on Rydberg blockade, Ph.D. thesis, Technische Universität München, 2014.
- [14] I. Mirgorodskiy, F. Christaller, C. Braun, A. Paris-Mandoki, C. Tresp, and S. Hofferberth, Electromagnetically induced transparency of ultra-long-range Rydberg molecules, *Phys. Rev. A* **96**, 011402 (2017).
- [15] J. Lampen, H. Nguyen, L. Li, P. R. Berman, and A. Kuzmich, Long-lived coherence between ground and Rydberg levels in a magic-wavelength lattice, *Phys. Rev. A* **98**, 033411 (2018).
- [16] D. Tiarks, S. Schmidt-Eberle, T. Stolz, G. Rempe, and S. Dürr, A photon-photon quantum gate based on Rydberg interactions, *Nat. Phys.* **15**, 124 (2019).
- [17] Y. M. Hao, G. W. Lin, K. Xia, X. M. Lin, Y. P. Niu, and S. Q. Gong, Quantum controlled-phase-flip gate between a flying optical photon and a Rydberg atomic ensemble, *Sci. Rep.* **5**, 10005 (2015).
- [18] S. Das, A. Grankin, I. Iakoupov, E. Brion, J. Borregaard, R. Boddeda, I. Usmani, A. Ourjoumtsev, P. Grangier, and A. S. Sørensen, Photonic controlled-PHASE gates through Rydberg blockade in optical cavities, *Phys. Rev. A* **93**, 040303 (2016).
- [19] A. C. J. Wade, M. Mattioli, and K. Mølmer, Single-atom single-photon coupling facilitated by atomic-ensemble dark-state mechanisms, *Phys. Rev. A* **94**, 053830 (2016).
- [20] L.-M. Duan, M. D. Lukin, J. I. Cirac, and P. Zoller, Long-distance quantum communication with atomic ensembles and linear optics, *Nature (London)* **414**, 413 (2001).
- [21] N. S. Ginsberg, S. R. Garner, and L. V. Hau, Coherent control of optical information with matter wave dynamics, *Nature (London)* **445**, 623 (2007).
- [22] B. Zhao, Y.-A. Chen, X.-H. Bao, T. Strassel, C.-S. Chuu, X.-M. Jin, J. Schmiedmayer, Z.-S. Yuan, S. Chen, and J.-W. Pan, A millisecond quantum memory for scalable quantum networks, *Nat. Phys.* **5**, 95 (2008).
- [23] S. D. Jenkins, T. Zhang, and T. A. B. Kennedy, Motional dephasing of atomic clock spin waves in an optical lattice, *J. Phys. B* **45**, 124005 (2012).
- [24] S. Kuhr, W. Alt, D. Schrader, I. Dotsenko, Y. Miroshnychenko, A. Rauschenbeutel, and D. Meschede, Analysis of dephasing mechanisms in a standing-wave dipole trap, *Phys. Rev. A* **72**, 023406 (2005).
- [25] F. Yang, T. Mandel, C. Lutz, Z.-S. Yuan, and J.-W. Pan, Transverse mode revival of a light-compensated quantum memory, *Phys. Rev. A* **83**, 063420 (2011).
- [26] G. Afek, J. Coslovsky, A. Mil, and N. Davidson, Revival of Raman coherence of trapped atoms, *Phys. Rev. A* **96**, 043831 (2017).
- [27] U. Ernst, A. Marte, F. Schreck, J. Schuster, and G. Rempe, Bose-Einstein condensation in a pure Ioffe-Pritchard field configuration, *Europhys. Lett.* **41**, 1 (1998).
- [28] B. Arora and B. K. Sahoo, State-insensitive trapping of Rb atoms: Linearly versus circularly polarized light, *Phys. Rev. A* **86**, 033416 (2012).
- [29] M. Saffman and T. G. Walker, Analysis of a quantum logic device based on dipole-dipole interactions of optically trapped Rydberg atoms, *Phys. Rev. A* **72**, 022347 (2005).
- [30] See Supplemental Material at <http://link.aps.org/supplemental/10.1103/PhysRevA.101.013421> for modeling details and experimental details.
- [31] S. Zhang, F. Robicheaux, and M. Saffman, Magic-wavelength optical traps for Rydberg atoms, *Phys. Rev. A* **84**, 043408 (2011).
- [32] L. Li, Y. O. Dudin, and A. Kuzmich, Entanglement between light and an optical atomic excitation, *Nature (London)* **498**, 466 (2013).
- [33] M. J. Piotrowicz, M. Lichtman, K. Maller, G. Li, S. Zhang, L. Isenhower, and M. Saffman, Two-dimensional lattice of blue-detuned atom traps using a projected Gaussian beam array, *Phys. Rev. A* **88**, 013420 (2013).
- [34] D. Tiarks, S. Schmidt, G. Rempe, and S. Dürr, Optical  $\pi$  phase shift created with a single-photon pulse, *Sci. Adv.* **2**, e1600036 (2016).
- [35] M. Lewenstein, B. Kraus, J. I. Cirac, and P. Horodecki, Optimization of entanglement witnesses, *Phys. Rev. A* **62**, 052310 (2000).
- [36] A. V. Gorshkov, A. André, M. Fleischhauer, A. S. Sørensen, and M. D. Lukin, Universal Approach to Optimal Photon Storage in Atomic Media, *Phys. Rev. Lett.* **98**, 123601 (2007).
- [37] R. Jozsa, Fidelity for mixed quantum states, *J. Mod. Opt.* **41**, 2315 (1994).
- [38] M. Naraschewski and R. J. Glauber, Spatial coherence and density correlations of trapped Bose gases, *Phys. Rev. A* **59**, 4595 (1999).

- [39] S. Riedl, M. Lettner, C. Vo, S. Baur, G. Rempe, and S. Dürr, Bose-Einstein condensate as a quantum memory for a photonic polarization qubit, *Phys. Rev. A* **85**, 022318 (2012).
- [40] E. W. Hagley, L. Deng, M. Kozuma, M. Trippenbach, Y. B. Band, M. Edwards, M. Doery, P. S. Julienne, K. Helmerson, S. L. Rolston, and W. D. Phillips, Measurement of the Coherence of a Bose-Einstein Condensate, *Phys. Rev. Lett.* **83**, 3112 (1999).
- [41] N. Navon, A. L. Gaunt, R. P. Smith, and Z. Hadzibabic, Critical dynamics of spontaneous symmetry breaking in a homogeneous Bose gas, *Science* **347**, 167 (2015).
- [42] R. Zhao, Y. O. Dudin, S. D. Jenkins, C. J. Campbell, D. N. Matsukevich, T. A. B. Kennedy, and A. Kuzmich, Long-lived quantum memory, *Nat. Phys.* **5**, 100 (2008).
- [43] C. W. Raman and N. S. Nath, The diffraction of light by high frequency sound waves: Part I., *Proc. Ind. Acad. Sci.* **2**, 406 (1933).
- [44] C. S. Adams, M. Sigel, and J. Mlynek, Atom optics, *Phys. Rep.* **240**, 143 (1994).
- [45] R. Grimm, M. Weidemüller, and Y. B. Ovchinnikov, Optical dipole traps for neutral atoms, in *Advances in Atomic, Molecular, and Optical Physics* (Academic, San Diego, 2000), Vol. 42, pp. 95–170.